University of Stavanger

Faculty of Science and Technology

MASTER'S THESIS

Study program/ Specialization: **MSc in Petroleum Engineering**	Spring semester, 2012 **Restricted Access**
Writer: **Surya Dharma**	..... (Writer's signature)

Faculty supervisor: **Professor Aly Anis Hamouda (UiS)**

External supervisors: **Lilly Skatveit Bergsvik (BP)**

Andreas Burgos (Acona Wellpro)

Title of thesis:

Analyzing Vertical Lift Performance in a Complex Gas Lift Well Geometry

Credits (ECTS): **30**

Key words: **J-shaped well, gas lift, well geometry, transient reservoir behavior, hydrostatic head, steady state simulation, dynamic simulation**	Pages : 62 pages + Front part : 9 pages + Appendixes : 8 pages + CD Stavanger, 15th of June 2012

ABSTRACT

This study mainly investigates the vertical lift performance in a complex gas lift well geometry. Prosper is used to do gas lift design. OLGA is used to analyze the dynamic well behavior based on the gas lift design from Prosper. The study is started by analyzing the effect of well geometry by comparing the J-shaped well to the horizontal well with and without gas lift. It is continued by analyzing the effect of gas lift to well performance and startup behavior of the J-shaped well. The sensitivity of reservoir pressure, productivity index, water cut and surface casing pressure is covered in this study. In the last part of this study, transient reservoir behavior is covered to optimize classic gas lift design. Steady state and dynamic simulations are performed to fulfill the objectives of this study.

The J-shaped well demonstrates unfavorable behavior compared to horizontal well. The J-shaped well is prone to slugging behavior. To properly evaluate the possibility of producing a well without the aid of gas lift, it is recommended to simulate the segregation during shut in and following by startup/unloading sequence. Otherwise, the steady state simulation result can be misleading because it does not model the dynamic behavior during unloading. Gas lift can extend the lifetime of well with strong transient reservoir behavior. Gas lift can increase the regularity wells with cyclic behavior. In terms of stability, gas lift well can mitigate the instability. However, a large amount of gas lift is required to stabilize the flow. Steady state simulation is currently the standard technique utilized to do classical gas lift design. Dynamic/transient simulation is recommended for validation purposes of gas lift design intended for wells with complex well geometry. Modeling should be implemented in the future to engineer/design gas lift solution for wells with complex well geometry.

ACKNOWLEDGEMENTS

In the name of Allah, the Most Gracious and the Most Merciful

Alhamdulillah, all praises to Allah for the strengths and His blessing in completing this thesis. Special sincere appreciation and gratitude goes to my academic supervisor Professor Aly Anis Hamouda for his excellent dedicated supervision and kind suggestion throughout this thesis work.

The thesis work was carried out at BP Norge premises in the period of January – June 2012. I would like to express my sincere thanks to Lilly Skatveit Bergsvik and Andreas Burgos for their kind assistance and valuable support for my successful completion of this thesis work. I would also like to thank to my colleagues in BP Norge (Knut Tørlen, Jan Klepaker, and Bjørnar Tjøen) for their kind support during performing this challenging work.

I offer my regards and blessings to my friends who have done simulations and written their thesis in Gullfaks room. Alina Minikieva, Magnus Palm, Eirik Høvring, Gulnar and Rauan thank you for making a positive environment in the computer laboratory. I also wish to acknowledge the support provided by my best friend, Dwayne Martin. I thank to all my Indonesian friends (Sanggi, Sakti, Tomy, Kriswandani, Yahya, Hermanto, dan Whida).

I am heartily thankful to my lovely wife and daughter, Annisa Solihah and Fatimah Aurora Azzahra for their support and encouragement throughout my study. My parents, Hadi Soepomo and Rosmalawaty, receive my deepest gratitude and love for their dedication and the many years of support during all of my studies that provided the foundation for this work. Last but not least, to those who indirectly contributed in this thesis, your kindness means a lot to me. Thank you very much.

Surya Dharma, June 2012

LIST OF CONTENTS

LIST OF FIGURES

LIST OF TABLES

1 INTRODUCTION

1.1 BACKGROUND INFORMATION

The Valhall field is one of the fields that are operated by BP Norge that has been produced since 1982. The field is a North Sea Chalk field producing from Tor and Lower Hod Formations. The field is originally developed with three facilities (Quarter Platform, Drilling Platform, and Production Platform) but now the complex consists of five separate steel platforms that are bridge-connected. To provide efficient access to the flank area in the North and South of the field, installation of two new wellhead platforms were approved in 2001. These two unmanned flank platforms are around 6 kilometers from the field centre.

The Valhall field is produced based on the depletion and compaction drive mechanism. Water injection is recently implemented to increase the oil recovery and pressure maintenance in the reservoir. Low reservoir pressure has led to cyclic performance and low uptime. Gas lift is being implemented to secure high uptime and continuous production from wells. Gas lift design is challenging because of the complexity of the well geometry of the well (J-shaped). A strong transient reservoir behavior with the uncertainty of the drainage area also gives more challenge for optimizing a gas lift design.

This thesis will study the influence of certain aspects that affects gas lift design such as well geometry, transient reservoir behavior, and inter relation between steady state and dynamic modeling.

1.2 PROJECT OBJECTIVES AND SCOPE OF WORK

The detail objectives of this thesis are:

- Model transient and steady state performance of gas lift well with complex well geometry using OLGA.
- Validate steady state and transient models to field data.
- Analyze effects of well geometry (J-shaped in well) and gas lift on well performance.
- Describe startup challenges in complex well geometry and gas lift wells.
- Study effects of transient reservoir behavior with and without the use of gas lift.

This thesis is divided into six chapters.

Chapter 2 introduces some concepts and terms that used in this thesis such as gas lift, vertical lift performance, instability, gas lift valve characteristics (orifice versus nozzle-venturi), and slugging behavior.

Chapter 3 provides some information about Valhall field, flank gas lift, challenges, and S-02 well that is used to model the vertical lift performance in a complex gas lift well geometry. S-02 well is used to model this phenomenon as this well has the highest transient reservoir behavior and the most complex gas lift well geometry.

Chapter 4 studies detailed modeling using steady state (Prosper) and dynamic simulator (OLGA). The model has been validated by comparing downhole gauge pressure measurements to calculated pressure at the same depth. J-shaped and horizontal wells are modeled to study the effect of well geometry. Sensitivities of reservoir pressure, productivity index, and water cut are performed to study the expected behavior of S-02 well over time. Gas lift and transient behavior cases are modeled to study the well and startup performance. Gas lift after the well is shut in is modeled to study the effectiveness of gas lift. Sensitivity of casing pressure in the gas lift well is added to study the optimized casing pressure for gas lift operation.

Chapter 5 discusses the results from chapter 4. The effect of well geometry and gas lift are discussed especially during startup. Well instability and transient reservoir behavior are also covered in this chapter. Chapter 6 includes the conclusions of this thesis.

2 THEORY AND LITERATURE SURVEY

2.1 GAS LIFT CONCEPT

Gas lift is a method of artificial lift that uses gas as an external source for increasing the gas liquid ratio to lift the well fluids. The primary objective of gas lift system is to help lifting the fluid and to increase the production. The concern of implementing gas lift system is the availability of the gas. Since gas lift is operated at relatively high pressure, compression of gas lift is needed to ensure the gas is received in a well at the design pressure.

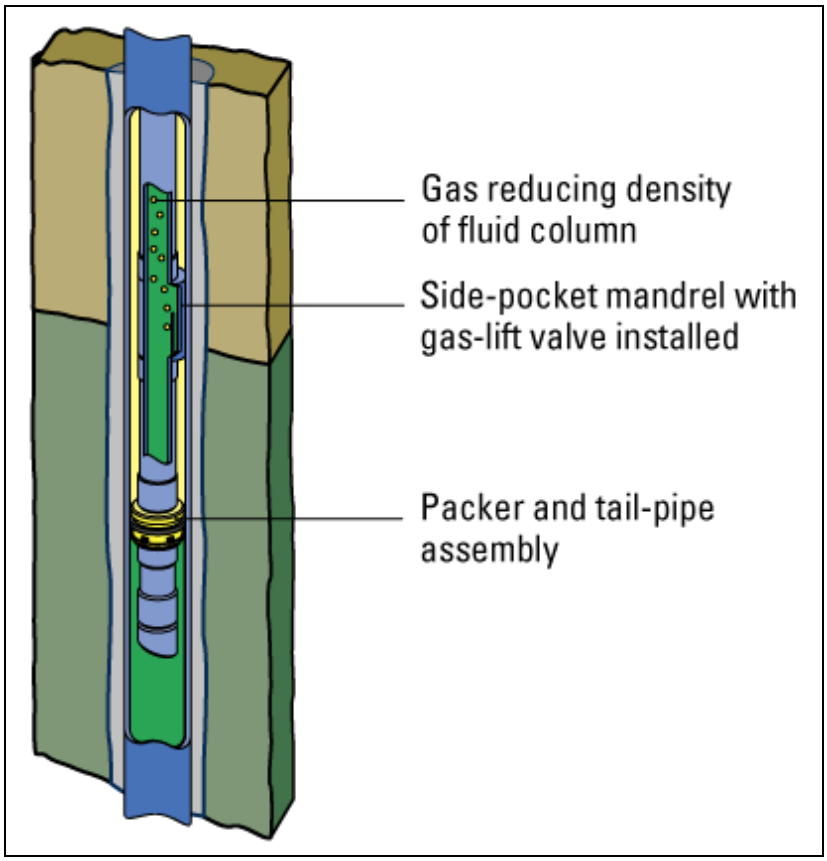

Figure 1 Gas Lift System. Courtesy of Schlumberger Oilfield Glossary

Gas is injected to the annulus into the maximum depth on a basis of the available gas injection pressure. The injected gas mixes with the produced fluid from the formation and decrease the flowing pressure gradient of the mixing fluid from the injected depth up to the surface. The decrease of pressure gradient establishes the higher bottomhole drawdown. So, gas lift can increase the production of the well.

There are two types of gas lift; intermittent gas lift and continuous gas lift. Intermittent gas lift is used for the removal of slug fluid in oil and gas wells. It is commonly used to dewater the gas

wells. In this thesis, gas lift that will be discussed is continuous gas lift. All cases and discussion are not applied for intermittent gas lift.

2.2 VERTICAL LIFT PERFORMANCE

Vertical lift performance represents a process to flow reservoir fluids from bottomhole to a surface facility. Complexity of the vertical lift performance depends on phases of the fluid. Single phase flow model gives simpler calculation than the multiphase flow because it is dealing with flows of gas-liquid mixture.

In multiphase vertical flow, pressure is required to know to lift the fluids from the reservoir at a given rate from a given depth with a given gas-liquid ratio through tubing of a given size. The bottomhole pressure must be sufficient not only to overcome flow resistance along the tubing and the surface choke (friction) but also sufficient to support the hydrostatic head based on the total weight compressible mixture in the tubing (gravity). The pressure drop due to acceleration is also considered as a result of expansion of fluids as the pressure reduces. In single-phase horizontal flow, the total pressure drop for a given flow rate can be represented as so many pounds per square inch per thousand feet of length. It is difficult for the vertical two phase flow because the pressure drop per unit length is not constant, but increases with depth.

For oil wells, the main component of pressure loss is the gravity or hydrostatic term. Gilbert[3] expresses the vertical lift performance that calculation of hydrostatic pressure loss requires knowledge of the proportion of the pipe occupied by liquid (holdup) and the densities of the liquid and gas phases. Accurate modeling of fluid PVT properties is essential to obtain in-situ gas/liquid proportions, phase densities and viscosities. Calculation of holdup is complicated by the phenomenon of gas/liquid slip. Gas, being less dense than liquid, flows with a greater vertical velocity than liquid. The difference in velocity between the gas and liquid is termed the slip velocity. They are therefore more correctly termed 2-phase flow correlations. Depending on the particular correlation, flow regimes are identified and specialized holdup and friction gradient calculations are applied for each flow regime.

2.3 INSTABILITY

This sub chapter includes a summary of a literature survey that related to instability of gas lift operation as a core subject in order to understand vertical lift performance. In the beginning, the definition of instability is discussed in terms of gas lift operation. Then, gas lift criterion by Asheim[1] is discussed as a parameter of instability in one of the software that is used in this thesis. The instability criterion by Asheim is used in this thesis as a result of steady state

modeling by Prosper. To understand the microscopic point of view, this thesis will discuss about casing heading and density wave behavior that can affect the instability of the gas lift. Gas lift valve performance curve will also covered in this thesis as this factor seems affect the instability of the gas lift operation. In this thesis, the dynamical simulation by OLGA is used to understand the casing heading instability and density wave behavior.

Another term that will be used in this thesis is regularity. Regularity is used for the cyclic well to exhibits how often the well is produced during certain period.

2.3.1 Instability Definition

To understand the gas lift behavior in the complex well geometry, Instability is one of the most important factors that will be discussed in this thesis. There are two types of Instability in this thesis; static or steady state instability and dynamic instability. Figure 2 illustrates the behavior of those two instabilities.

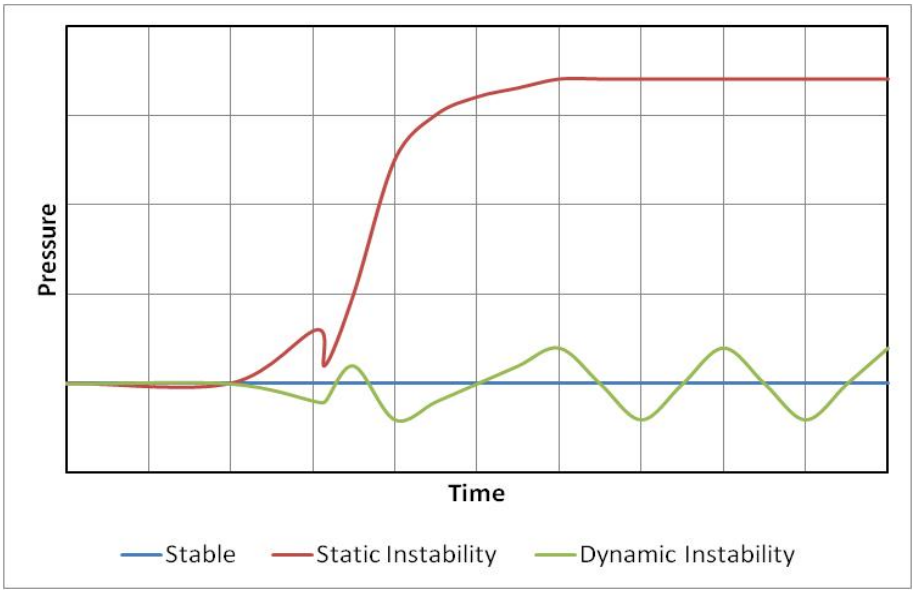

Figure 2 Illustration of Stability Concept[2]

Static instability happens when a new steady state condition is applied as a change to reach stable condition. Theoretically, the new steady state condition can be predicted using the law of the steady state flow. As a result, a static instability can lead either to a different steady state condition or to periodic behavior (dynamic instability). Xu and Golan[2] express this behavior as a left hand intersection in the IPR and VLP cross section graph.

Dynamic instability happen[2] when the inertia and feedback effects have an essential part of the process. In such cases, the system continues to alternate about an average level in a

periodic manner. An example of dynamic instabilities is casing heading in flowing wells due to time lag between the release and accumulation of gas in the annulus of the well.

The instability can be analyzed using the liquid fraction distribution along the well which is called holdup in this study. The instability of the pressure usually corresponds to a certain holdup. By analyzing the holdup along the time, it will be easier to understand the well behavior. OLGA has a 2D holdup result that can be used to understand the 2D physical behavior of the well.

2.3.2 Inflow Response

Asheim[1] introduced stability criteria as a result of the inflow responses of reservoir fluid and lift gas. The inflow rate which is heavier fluid that comes from the reservoir is more sensitive to pressure behavior than the gas lift flow rate. The mixture of flowing fluid from formation and injected gas will decrease the average density that increase in response to decrease in tubing pressure. To stabilize the flow, the source from the formation will tend to change back the condition that causes the tubing pressure to increase again.

$$F_1 = \frac{\rho_{gsc} B_g q_{gsc}^2}{q_{Lsc}} \frac{J}{(EA_i)^2} > 1$$

By this criterion, stability is affected by a high flow rate of lift gas, a high productivity index, and a small injection port. Gas lift is considered as a stable flow when F_1 is higher than 1.

2.3.3 Pressure Depletion Response

If the 1st order of stability criterion is not fulfilled, the tubing pressure that decreases because of the injected gas will cause the gas flow rate to increase more than the liquid flow rate from the formation. The increasing injected gas will decrease the tubing pressure. However, this also will cause the decreasing pressure of the annulus. The decreasing pressure of the annulus will cause the decreasing injected rate to the tubing when the decreasing pressure of the annulus is higher than the decreasing pressure of the tubing. The decrease of the differential pressure between annulus and the tubing will decrease the gas lift rate. This stabilizes the flow.

$$F_2 = \frac{V_t}{V_a} \frac{1}{gD} \frac{p_t}{(\rho_{fi} - \rho_{gi})} \frac{q_{fi} + q_{gi}}{q_{fi}(1 - F_1)} > 1$$

The 2nd order criterion, stability is affected by gas conduit volume, injected gas flowrate, 1st order stability criterion. A high tubing pressure that provided by higher wellhead backpressure, will be stabilizing if the downhole gas injection volume is maintained constant. Gas lift is considered as a stable flow when F_2 is higher than 1.

2.3.4 Casing Heading Instability

Casing heading behavior was firstly introduced by Bertuzzi[3] in 1953. Xu and Golan[2] explain the casing head as an oscillating sequence. The casing heading is caused by relationship between pressure and gas injection rate either in the tubing and/or the annulus. A decrease in the tubing pressure at the injection depth will cause flowing of higher gas injection. The pressure in the annulus will start to drop because of the higher gas injected. Due to the time delay between the change in the downhole discharge rate and surface injection rate, the flow may start to oscillate about the design rate. This condition sometimes will cause the well to die. Xu and Golan[2] describe the oscillating sequence in the following steps.

1. Start at the gas injection point. A sudden reduction of tubing flow pressure results in more gas discharge through the downhole orifice.
2. More gas discharge will further reduce the flowing pressure, promoting more gas flowing through the downhole orifice.
3. Since the gas supply through the surface choke cannot meet in time the higher gas rate discharge into the production string, the casing head pressure eventually decrease. This results in a decrease of gas flow into the tubing.
4. The tubing flowing pressure starts now to increase because of the gas injection reduction. This accelerates the reduction of gas injection into the tubing.
5. The trend now is swayed to opposite. Because of higher tubing flowing pressure and lower upstream pressure, the downhole orifice can discharge less gas than the surface now supplies. The casing pressure begins to build up.
6. As the casing pressure is built up, gas rate into tubing starts to increase. More gas injection reduces the tubing flowing pressure and thus sways the flow condition back to step 3.

The level of instability depends on the amplitudes of rate and pressure fluctuations. From the operational stand point, choking the surface production facility is a very poor measure to stabilize gas lift production. Increasing the choke opening tends to stabilize the flow. But, it result to over injection gas which is undesirable.

2.3.5 Density Wave Instability

Oscillation sequence is also observed in a gas lift wells in North Sea when the well produced from depleted reservoirs. This happened on a gas lift wells that are already equipped with the nozzle type of venturi gas lift and it is observed that no pressure oscillation in the annulus. This type of instability is called "density wave" by Hu and Golan[6]. Since the gas injection rate is constant, then any variation in the liquid inflow to the wellbore will easily result in the density change of the two phase mixtures in the tubing due to the change of phase fraction. Clearly, the mixture density change will result in the change of hydrostatic pressure drop, thus the total pressure drop, particularly in a gravity dominating system. The initiated mixture density change due to phase fraction variation at the bottom of the well will travel along the tubing as density wave, which sometimes is also called continuity wave or void wave. This density wave does not necessary introduce instability to the system since the well has a self-controlling effect. This means that any increase in the pressure drop due to an increase in mixture density will result in the reduction of the liquid inflow and thus the mixture density, and vice versa. But this self controlling mechanism is more or less delayed due to the out of phase effect between the well influx and the total pressure drop along the tubing. To a certain level, it breaks down and the well becomes unstable.

2.4 GAS LIFT VALVE

2.4.1 Gas Lift Valve Performance

Gas lift valve performance is defined by Decker[4] as the quantitative measure of a valve's flow rate response to changes in casing and/or tubing pressure for a given set pressure. Most gas lift manufacture will provide the gas lift performance curve to express the performance of the gas lift valve.

The American Petroleum Institute (API's)[5] recommended method of spacing and sizing gas-lift-valve ports is published in API's Recommended Practice (RP) 11V6 Design of Continuous Flow Gas Lift Installations Using Injection Pressure Operated Valves (1992). This recommended practice describe the design technique that has been used for many years with considerable success and uses the Thornhill Craver (TC) equations and charts as the principal methods of sizing gas-lift-valve ports.

There are several assumptions with the use of TC chart that described by the American Petroleum Institut[5]. First, it assumes that the valve port is fully open, and second, it assumes an unobstructed flow path through the valve. Both of these assumptions could be incorrect,

depending on the type of gas lift valve used and the pressure being applied to the bellows. Every Injection Pressure Operated (IPO) gas lift valve has a property called loadrate. This property refers to the amount of opening a valve will achieve for a given annulus and tubing pressure. In most cases, a gas lift valve is rarely fully open when passing gas. Secondly, the valve and/or stem, downstream restrictions and the reverse-flow check usually obstruct the flow passage through a gas lift valve. Based on these two conditions, the gas lift flow rate through the valve is actually less than the result from the TC equations; and some companies use a safety factor to represent these conditions. Correlations of predicting the gas passage rate based on the specific pressure and temperature condition is made by license through the Valve Performance Clearinghouse™. In this thesis, the gas lift valve performance data are generated from the VPC™ using the demo gas lift valve from SPT Group.

2.4.2 Nozzle-Venturi Valve

Nozzle-Venturi gas lift valve is a type of continuous gas lift valve that replaces an orifice valve. This valve minimizes the casing heading problem in terms of subcritical gas flow through orifice. Basically it is similar to the orifice except that the flow control element is a converging-diverging Venturi device.

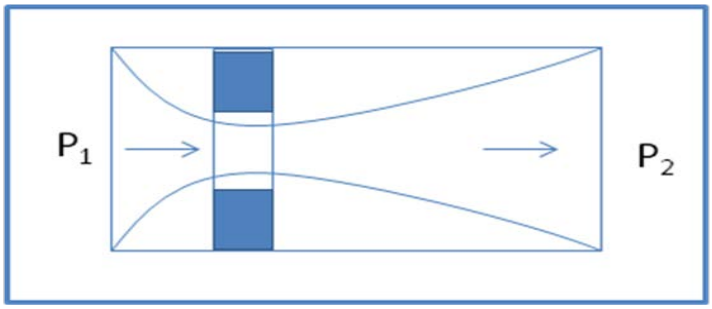

Figure 3 Cross Section of Orifice and Nozzle Venturi valve[15]

The comparison profile of orifice and nozzle venturi valve is shown in Figure 3. The orifice valve is represented by the two blue squares and the nozzle-venturi type is represented by the two curves converging-diverging venturi device. The pressure profile between nozzle-venturi valve and square-edged orifice is shown in the Figure 4.

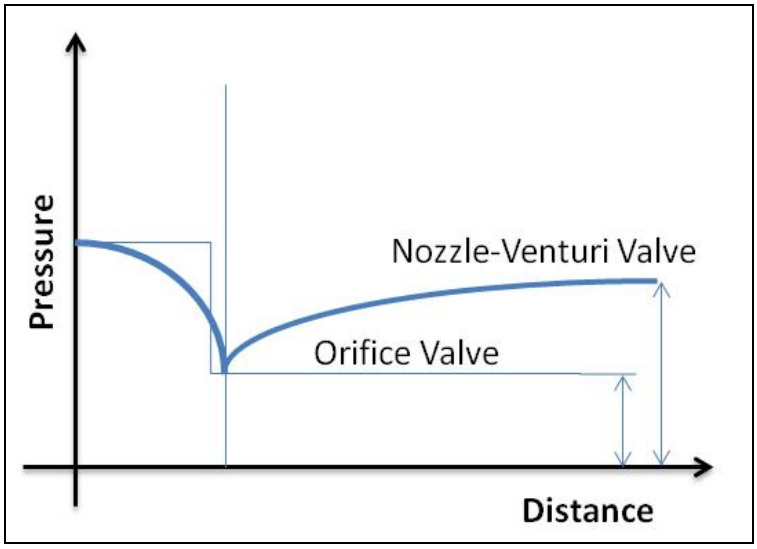

Figure 4 Pressure distributions in an orifice and Nozzle-Venturi valve[15]

It is assumed that critical flow with sonic velocity occurs in the throat section of both devices. In both of the valves, there is a decrease of a pressure along the flow path between the upstream and the downstream of the valves. However, nozzle-venturi valve can recover the decrease pressure that appears because of the restriction.

Figure 5 represents the gas passage characteristics of the orifice and the nozzle-venturi type where gas injection rates are plotted with tubing pressure at a constant injection pressure. Both valves have similar gas lift rate behavior where at the lower tubing pressure, the gas lift injection rate increases until the gas lift critical rate is achieved. However, the nozzle-venturi valve shows lower pressure differential between the injection and the tubing pressure than the orifice valve to achieve the critical rate. The nozzle venturi valve is very effective to prevent casing heading instability. Even the venturi type orifice is installed in the well; this study uses the orifice type of gas lift for the analysis.

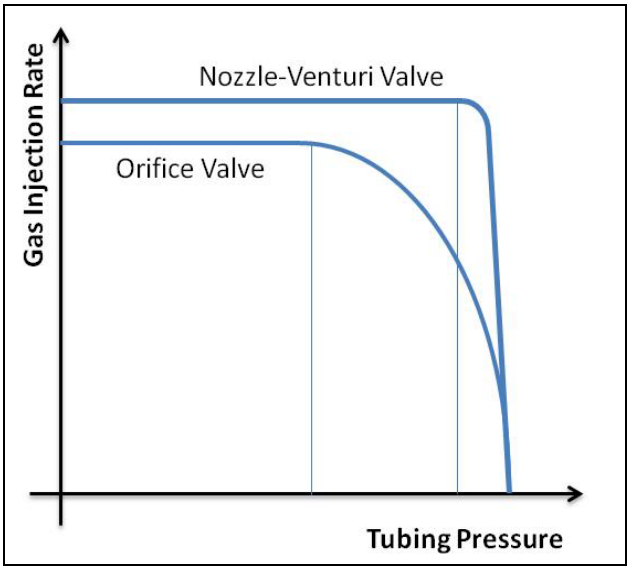

Figure 5 Comparison of gas passage characteristics of orifice and nozzle-Venturi gas lift valves[15]

2.5 TERRAIN SLUGGING

Norris[7] expresses when the gas and liquid flows in the well that fluctuations are sometimes caused by the slugging. Slugs may form as a result of hydrodynamic instability of a stratified flow. When the gas flows over a stratified liquid interface, it can generate waves, just as the air blowing over the ocean generates waves. If the amplitude of these waves becomes sufficiently large, they can bridge the pipe, and hydrodynamic slug can form. Hydrodynamic slugs are the most commonly encountered. They tend to be longer; the larger the pipe is and can, unfortunately, be thousands of feet long.

Because of pipeline terrain geometry, a more severe type of slugging can be built. In this terrain or "severe" slugging, J-section of the pipeline can develop liquid blockage. Because of this blockage, build up of hydrostatic head is developed from the two directions. The liquid holdup develops hydrostatic head in the downstream section where pressure buildup is developed as accumulation of gas pressure. The liquid will flow when the gas have sufficient pressure to push the liquid that accumulate along the J-section. The most dramatic example of terrain slugging occurs when a downwardly sloping pipeline terminates in a vertically profile of a well.

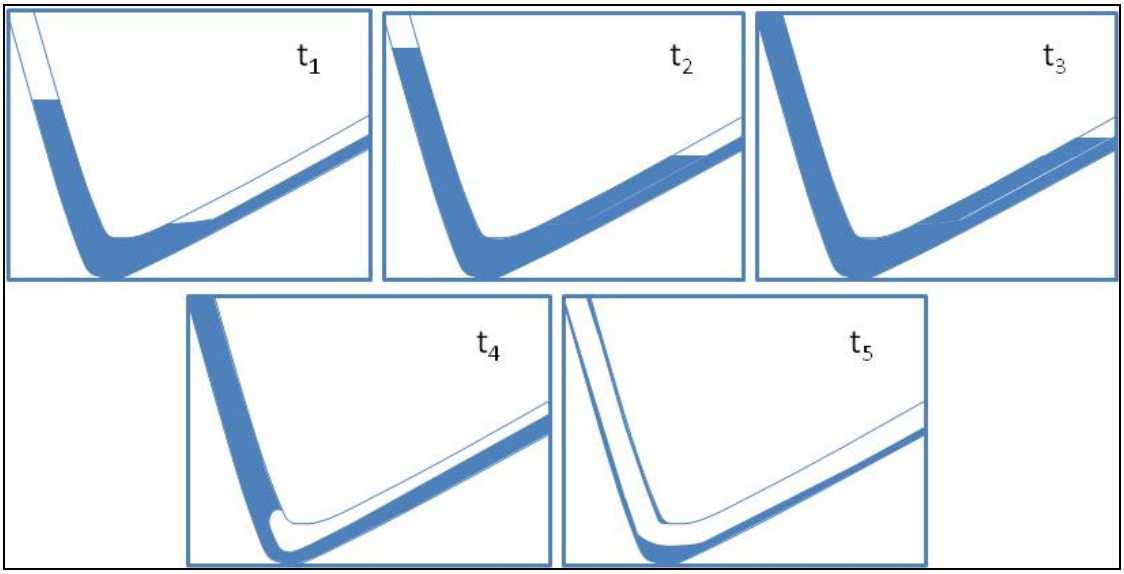

Figure 6 Stages for terrain slugging[14]

The complex well geometry (i.e: J-shaped well) has a risk of terrain slugging. The inclination greater than 90 deg seems to build accumulated volume in the lowest true vertical part of the well. The accumulated fluid will introduce high gravity dominated of the pressure drop. This phenomenon can block the flow of the fluids from the reservoir while building up the pressure downstream of the terrain slugging until certain pressure to kick off the accumulated liquid. The repetition will happen as a behavior of terrain slugging when the reservoir pressure in a near-bore area is not high enough against the liquid loading effect from the well.

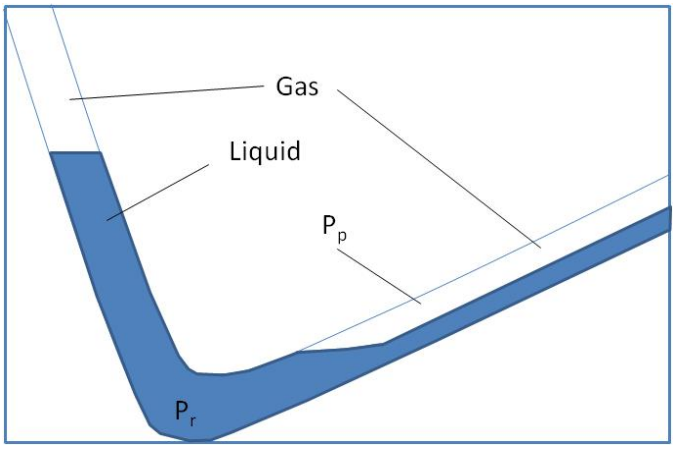

Figure 7 Terrain induced slugging in a riser

Considering Figure 7, severe slugging happened when the liquid prevents gas from passing the J-shaped section. This leads fluids are segregated along the riser and pressure build-up in the pipeline. The following conditions are fulfilled when the severe slugging presence:

- The stratified flow in the upstream pipeline is reached. The gas will be transported by the liquid around the J-shaped with the liquid. Segregated of the liquid establishes an effective blocking as the first criterion. This happened usually at low gas and liquid flow rates.
- When the J-shaped has been blocked, the hydrostatic pressure by the liquid in the riser increases faster than the gas compression pressure build-up in the pipeline. In order to keep the gas locked. This is expressed as

$$\frac{dP_r}{dt} > \frac{dP_p}{dt}$$

The higher hydrostatic pressure than the pipeline pressure blocks the fluids to be produced. So there will be less production during the buildup of the pipeline until the pipeline pressure is higher than the hydrostatic pressure. The fluid is produced intermittent as a result of a severe slugging.

3 CASE STUDY

This thesis studies the performance of the J-shape well (S-02) at the South Flank Platform in the Valhall field. The Valhall Field is located 290 km South West of Stavanger in the Norwegian corner between the Danish and British sectors. The Valhall field was discovered in 1975, after exploration drilling in the period of 1969 – 1974. The decision to develop the field was made in 1978 and the field started producing in October 1982. The crestal area of Valhall has two productive chalk zones, the Tor and the Hod formations. The Tor formation is the most productive, having porosities approaching 50%. Crestal areas of the Tor are found to be extensively fractured, resulting in dual porosity behavior with matrix permeability generally less than 10 mD. Production induced depletion resulted in high compaction rates associated with load transfer from the overpressured fluid to the ductile chalk matrix. This compaction drive has contributed to high primary recovery and has led to significant seabed subsidence. Through compaction has had a positive impact on recovery it has also resulted in drilling and well integrity challenges in the overburden.

The initial development consisted of a 3-platform complex (quarter platform, drilling platform, and process/compression platform) to provide additional slots for infill drilling. In 2000, the Valhall partnership approved a water injection program, from an additional Injection platform, IP. With continued subsidence, drilling wells in the overburden become increasingly difficult. To provide efficient access to the flank areas in the North and South, installation of two new wellhead platforms was approved in 2001. In line with the declining reservoir pressure in the Flank areas, it has been decided to implement gas lift in both platforms.

3.1 FLANK GAS LIFT AND CHALLENGE

The North and South Flanks are two satellite platforms located 6 km away from the main Valhall platform. Since the wells were originally brought online in 2003 and 2004, a decline in reservoir pressure has made it harder to produce from some of the wells. Today, many of the Flank wells are operated on a cyclical basis. After a period of flow that can extend for several weeks, each well is rested to allow the near well-bore region to re-pressurize. Knowing when to bring the well online is difficult. Attempts to bring the well online too soon can fail as the reservoir pressure is insufficient to get the well started. Each failed attempt will increase the amount of stripped oil, making subsequent attempts more difficult. On the other hand, waiting too long for the well to re-pressurize will have a significant impact on production.

The “J” shaped trajectory of the Flank wells makes them susceptible to slugging. In 2006, the BP slug controller was installed on a number of the wells with impressive results. Deployment of the controller led to an improvement in flow stability and an extended flowing period.

In light of the operational difficulties, gas lift has been installed on the Flank platforms. It is expected that the installation of gas lift will improve the ease of beaning up the Flank wells. Well availability should be improved significantly and the reduction in the hydrostatic head within the well should lead to higher production rates.

The introduction of gas lift should have a significant impact on well availability as it becomes easier to bring the wells online. Production rates will be higher as more wells can be flowed at any one time.

Compressed gas will be available at the Central Platform at a pressure of between 1475 and 1700 psig. An 8 inch pipe will be used to transport the compressed gas from the Central Platform to the Flank Platforms. Each well on the South and North Flank has been fitted with between three and four side-pocket mandrels.

Given the historical slugging within the well, there is a concern that the provision of gas lift may worsen the slugging. Fluctuations in the hydrostatic head during the slugging may lead to a variation in the gas lift injection point within the well. The bouncing of lift gas from one mandrel to another could further increase the level of instability. At worse, the gas lift system may assist the propagation of flow instabilities from one well to additional wells that would otherwise be stable.

Reducing the number of mandrels within each well has the potential to improve the level of stability during normal flowing conditions. At the same time, with fewer mandrels, the unloading of fluid during well startup will be much more critical. If the gas header pressure is insufficient to overcome the hydrostatic head within the well, it will be difficult to bean-up the well.

3.2 S-02 WELL

S-02 Well is one the wells in the South Flank platform. The well is located in the south west flank of the field. The well was drilled in February 2006. The well reaches 96.5 degree of inclination and 7301 m, MD is the longest well drilled on the Valhall field ever and also one of the longest horizontal sections at 2188 m MD. The following map shows the S-02 well position in the Valhall field.

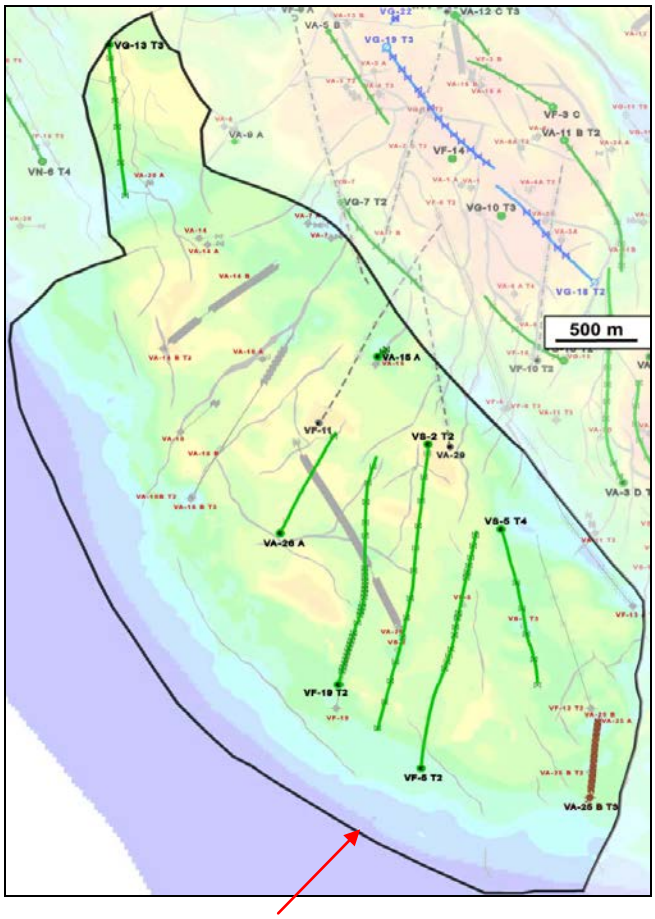

Figure 8 S-02 Well Position

The S-02 Well was completed by 4 ½" tubing tapered to 5-1/2" tubing. A tubing retrievable surface control subsurface safety valve was installed at 190 mMD and an annular safety valve was installed at 212 m MD. There are three side pocket mandrels in this well. Two mandrels were installed with the unloading valves and one mandrel was installed with the nozzle-Ventury type of valve (Stealth orifice) supplied by PTC. The following table shows the details data of gas lift valve in S-02 well.

Table 1 S-02 gas lift valve data

Depth	Valve Type	Port Size (64th in)	Opening CHP (barg)	Closing CHP (barg)	Design Flow Rate (MMscfd)
1104mMD	Unloader	10	116	114,7	0,55
2974mMD	Unloader	13	113	108,8	1,0
4164MMD	Stealth Orifice	19	107 (operating CHP)	n/a	3,0

Downhole pressure and temperature gauge was installed at 4200 m MD. This equipment provides real time pressure and temperature data as part of the well surveillance and monitoring

strategy in Valhall field. The well was perforated using 4 and 5 SPF with 180 deg of phasing. A total of 13 prop fracs were placed along the reservoir section during February and March 2006. The well was produced since March 2006 and the well has been in cyclic behavior since 2008. The well has high initial oil rate with rapid decline. Initial production of this well was around 6000 bopd with the peaked production around 7500 bopd and now still produces above 5000 bopd in a cyclical basis. The following profile shows the production profile of S-02 well since the well was produced at 2006.

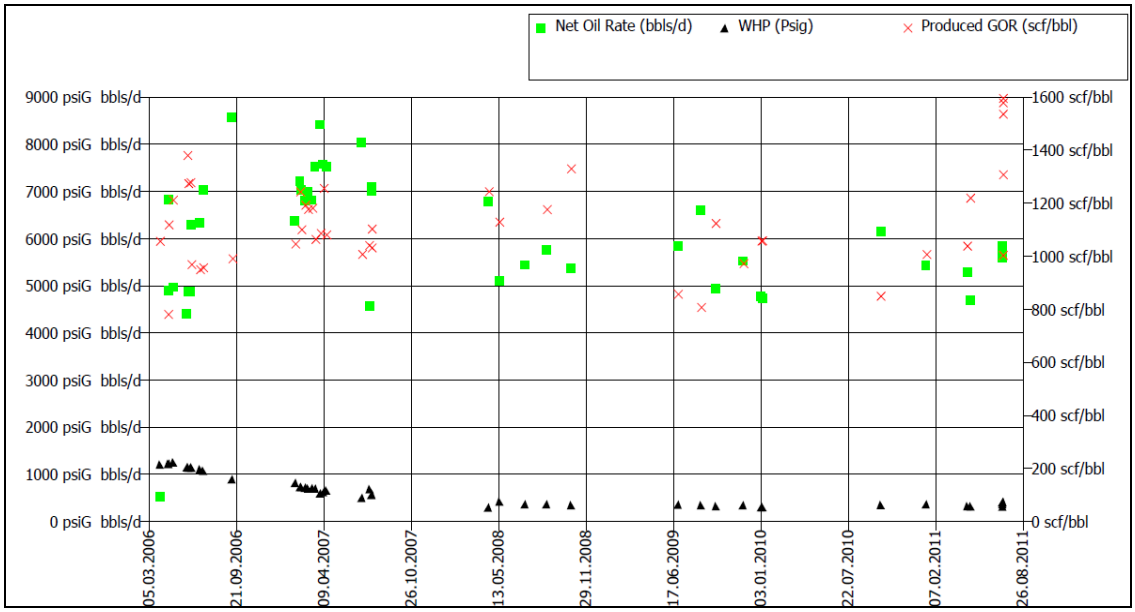

Figure 9 S-02 well production profile

From the production profile, the well was kept producing at around 5000 – 6000 bopd with the decline of wellhead pressure from 1200 psig in 2006 down to 300 psig in 2011. The GOR is quite stable at 1000 – 1200 scf/bbl.

3.3 GAS LIFT OPERATION IN S-02 WELL

In July 2011, the gas lift was first started in the well. The last gas lift operation is in January 2012. The figure below shows the trend of the well from October 2011 until February 2012.

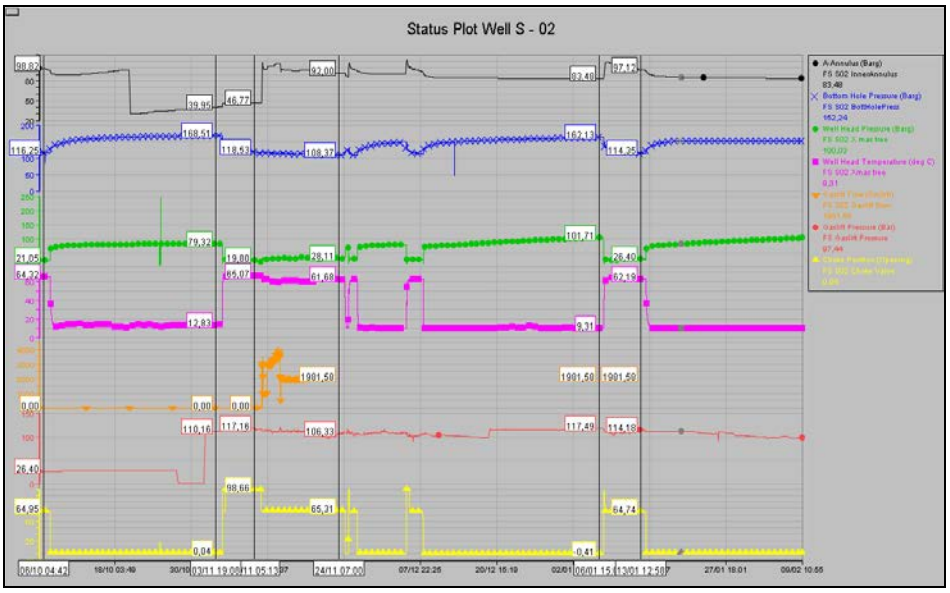

Figure 10 S-02 well behavior

In November 2011, the step rate test is performed in order to understand the gas lift behavior. At the startup period, the well produces naturally. After 5 days of production, the well is injected by gas lift at the casing pressure around 110 barg. From figure above, the detail parameters can be observed when the gas lift is injected. During the production, the gauge pressure was decreasing until the well shut in due to field shutdown. This behavior shows that this well has a strong transient behavior and the steady state is still not reached during 20 days of production. However, in the late time of the production, the decreasing of the reservoir pressure (0.2 bar/day) is not as high as the early time of the production (9.5 bar/day).

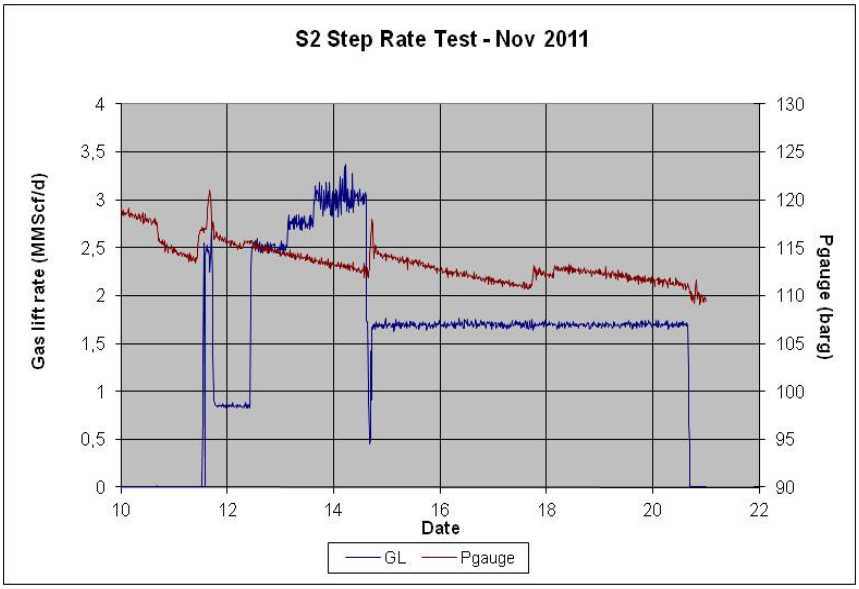

Figure 11 Gauge pressure and gas lift rate during production of S-02 well

The figure above shows the detail trend of gauge pressure when the gas lift is injected from the annulus. On 12th of November, the gas lift rate was increased from 0.8 MMscfd up to 2.5 MMscfd. On 13th of November, the gas lift rate was increased again to 2.7 MMscfd and 3 MMscfd. However, the gauge pressure did not show any strong response when the gas lift injection was increased.

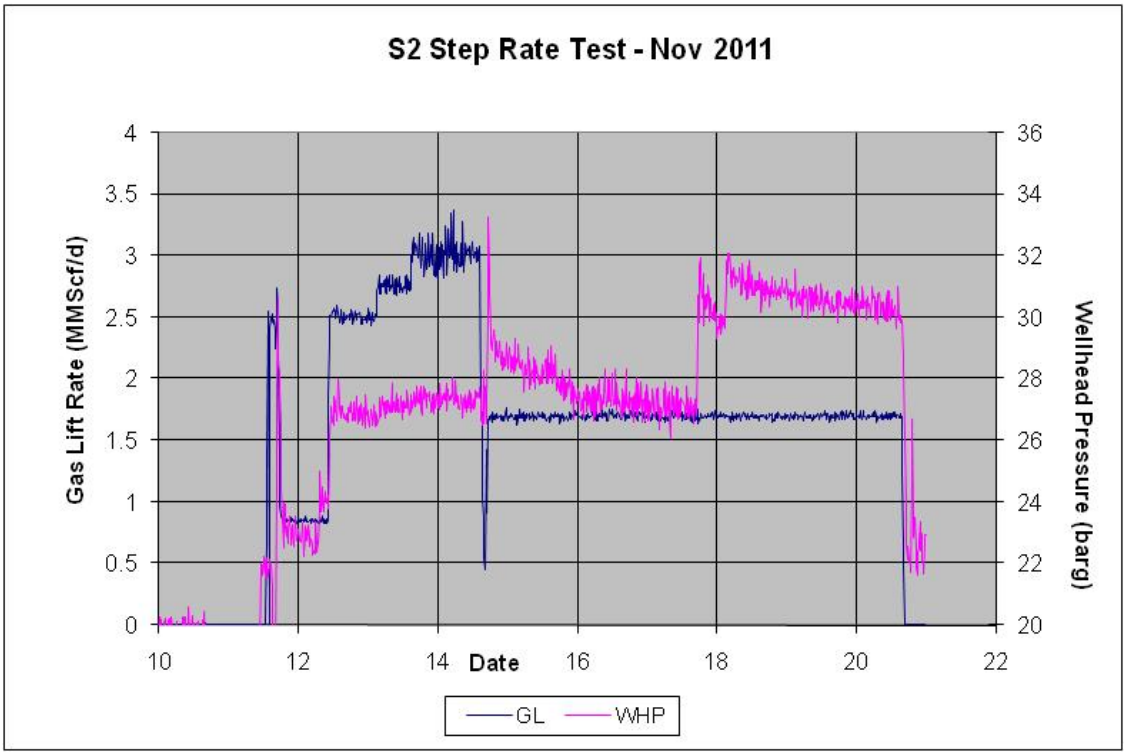

Figure 12 Wellhead pressure and gas lift rate during production of S-02 well

The figure above shows the response of wellhead pressure when changing the gas lift rate. On 12th of November, a response of wellhead pressure was increasing when the gas lift rate increased from 0.8 MMscfd up to 2.5 MMscfd. However, there is no significant response in the wellhead pressure when the gas lift rate was increased up to 2.5 MMscfd and 3 MMscfd. When the gas lift rate was decreased down to 1.7 MMscfd, a response of wellhead pressure can be seen even it was difficult to understand. From these two trends, there was a possibility that the gas lift rate at the injection depth did not respond immediately after the change of the gas lift rate at the different gas lift choke was happened.

It is also interesting to analyze the well behavior during the startup of the well. The figure below shows the startup of the well after around one month of shut in. Before the well is opened, the bottomhole pressure is relatively stable at the 168.7 barg and the wellhead pressure is stable at 79.4 barg. When the well is started-up, the bottomhole pressure gradually decreases. The

bottomhole pressure trend shows static instability behavior when the fluid from the reservoir pushes the accumulated liquid in the well. It indicates that some slugs produce in the beginning.

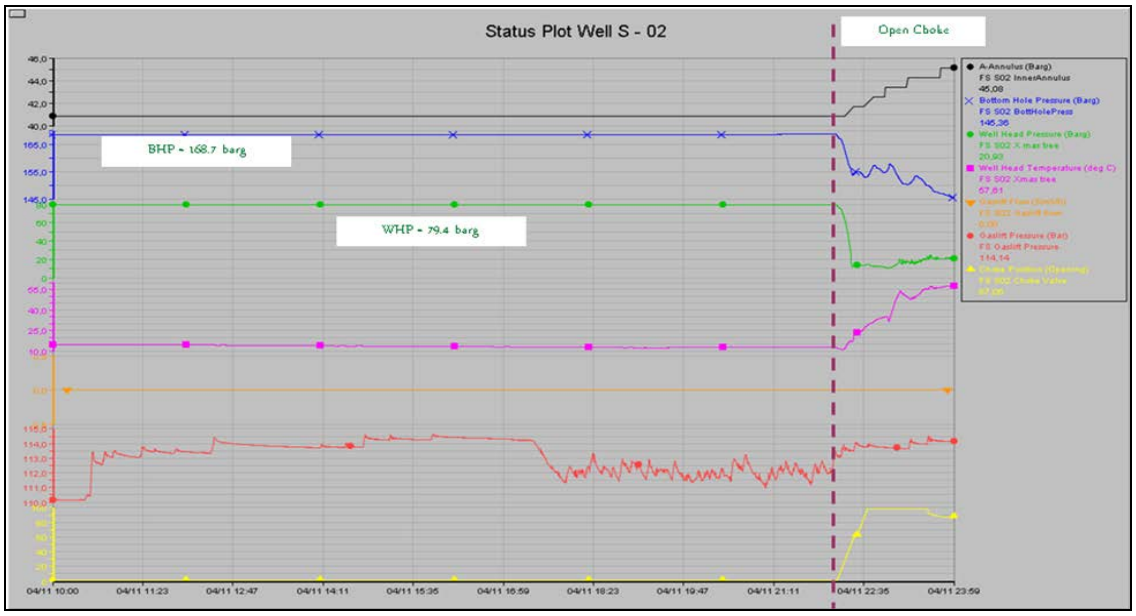

Figure 13 S-02 well behavior during startup on 4th November 2011

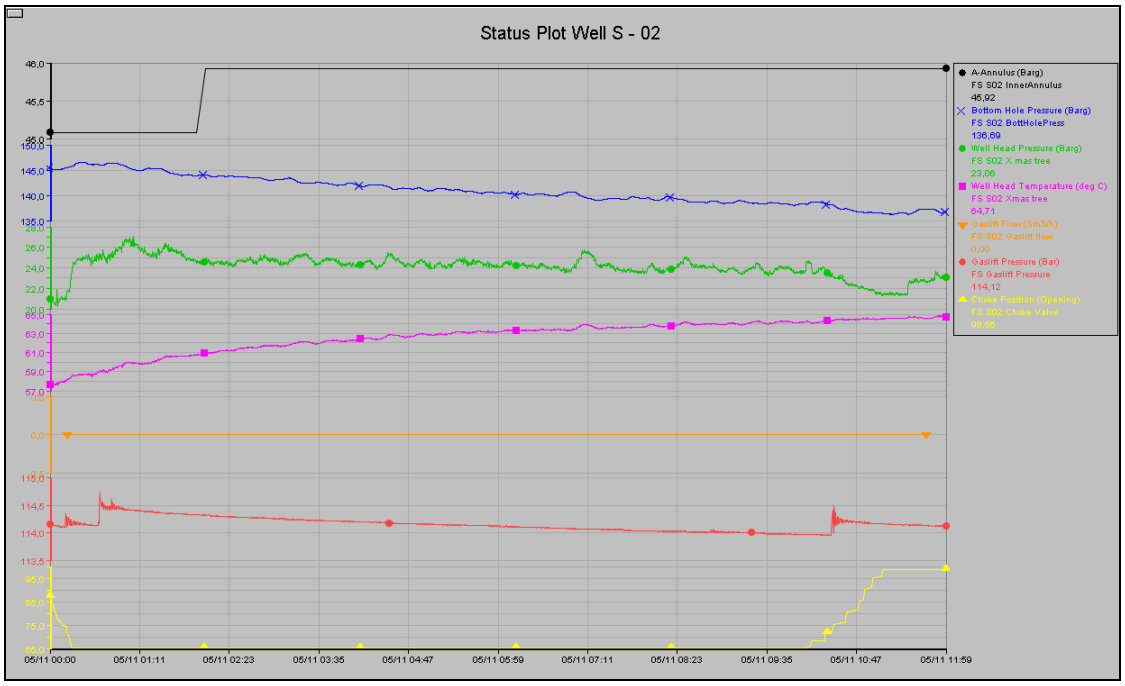

Figure 14 S-02 well behavior during startup on 5th November 2011

The well shows relatively stable behavior after around 3 hours of startup. The decreasing of the bottomhole pressure (for about 10 bar/day) shows the transient behavior of the well. Small fluctuation of wellhead pressure shows an indication of slug flow at the wellhead.

4 MODELING AND RESULTS

The aim of this study is to analyze the effect of well geometry and gas lift on well and startup performance. The steady state and dynamic modeling are used to understand the behavior and try to simulate the actual condition when the well is flowing naturally or using gas lift. Well modeling using Prosper and OLGA are used in this thesis. Prosper is used to model the steady state behavior and the instability criteria by Asheim[1]. OLGA is used to model the transient and dynamical behavior of gas lift operation. PVT sim is used to generate the PVT data for black oil model that used in OLGA. PVT data from PERA for black oil model is used to model the PVT data in PROSPER. Figure 15 shows the modeling and discussion flow chart including Prosper and OLGA modeling.

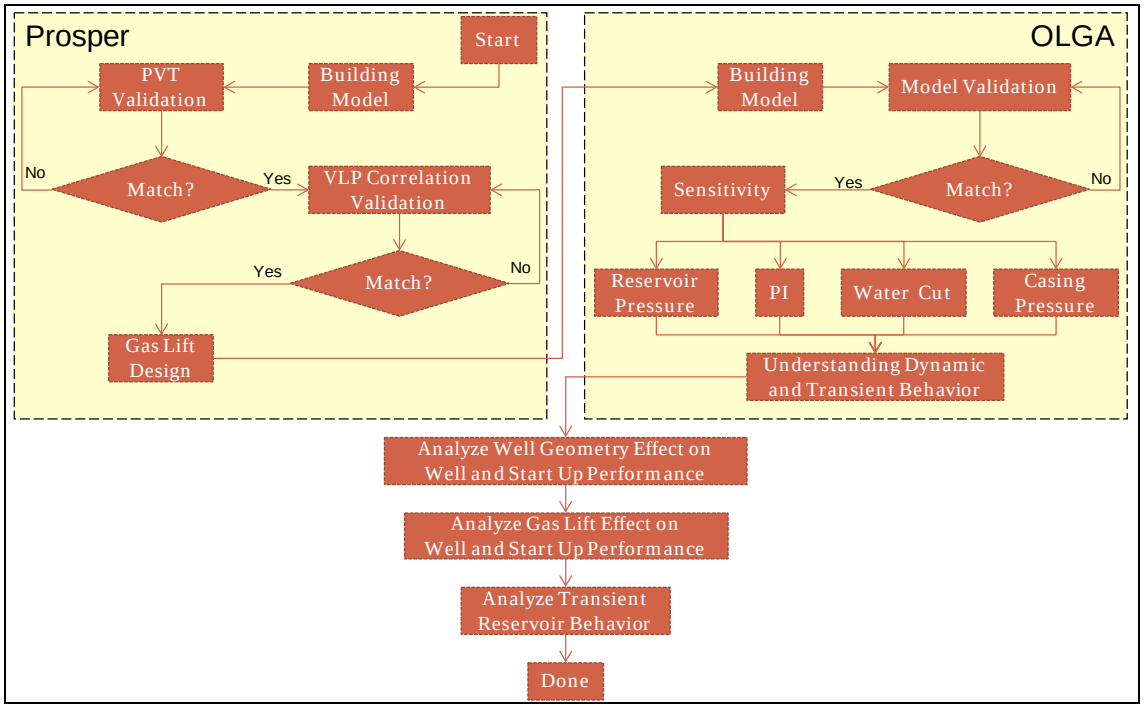

Figure 15 Modeling and discussion flow diagram

4.1 PROSPER MODELING

Prosper is used to model the gas lift well of S-02 well for steady state modeling. Prosper is a powerful software to model single well behavior. Black Oil model is used as a model to describe the fluid properties in PROSPER. Gas lift model is used as an artificial lift model with the type of friction loss in annulus to model the instability criteria. The well is completed using cased hole and perforated type and top of perforation is used as a bottomhole depth. The following figure shows the system summary of S-02 well model.

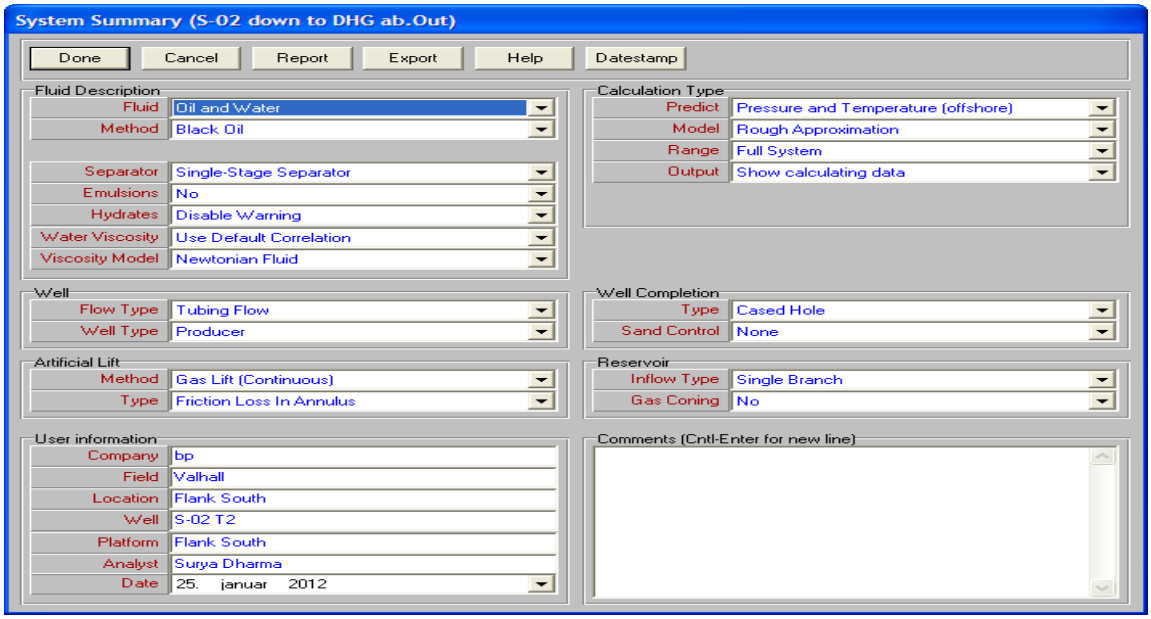

Figure 16 S-02 system summary

4.1.1 Model Development

4.1.1.1 PVT Data

Prosper used black oil model to simplify the PVT calculation in the model. A study had been conducted by PERA A/S to analyze all the available fluid data, including compositional analyses and PVT measurements, and well test data for the field. PERA generates black oil PVT tables that represent the PVT data for Valhall field. This table based on a "medium-GOR sample" is used in this model to match the PVT data that represent S-02 model.

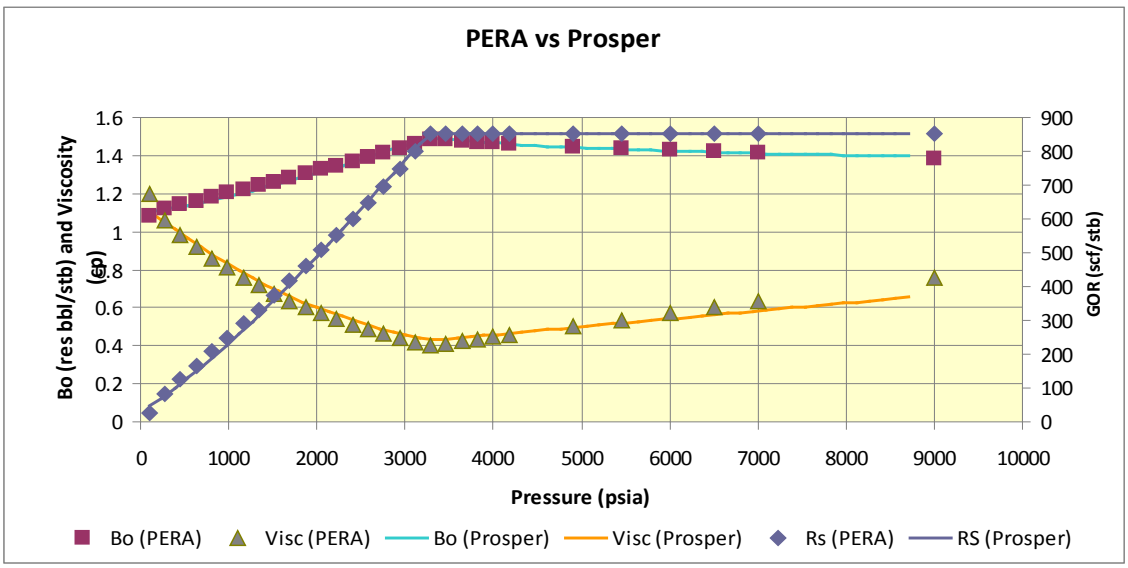

Figure 17 PVT validation to PERA model in Prosper

The figure above shows how PVT data from Prosper is being matched to the PERA data. 5 points are used to match the PVT data. From the matching process, Standing Correlation is used to calculate bubble point pressure, gas oil ratio, and formation volume factor while Beal et al correlation is used to calculate the oil viscosity.

4.1.1.2 Inflow Performance Relationship

Inflow performance relationship used Productivity Index (PI) as a reservoir model. Based on Schlumberger Oilfield glossary, Productivity Index is a mathematical means of expressing the ability of a reservoir to deliver fluids to the wellbore. The PI is usually stated as the volume per psi of drawdown at the sandface ((bbl/d/psi). In this model, the base PI that is used 11 bbl/d/psi. This PI is also used in OLGA modeling based on the reservoir pressure of 200 barg in S-02 well.

4.1.1.3 Vertical Lift Performance

Vertical lift performance in gas lift prosper model consists of two parts; continuous gas lift data and equipment data. Equipment data consist of 4 parts; deviation survey, downhole equipment, geothermal equipment, and average heat capacities. Deviation survey of S-02 well was used to represent the actual well. Since it is only limited 20 points that Prosper is able to consider, filtering of data is done as shown as in the following figure.

Figure 18 S-02 well directional survey filtering

The pink square point shows the actual of directional data. The purple diamond point represents the filter data that is used in the Prosper model. The blue triangles show the gas lift mandrels position in the well.

Downhole equipment is modeled based on the wellbore schematic. The geothermal gradient is modeled based on the offshore environment and the weather condition in the Norwegian continental shelf. The following figure shows the behavior of geothermal gradient in S-02 well.

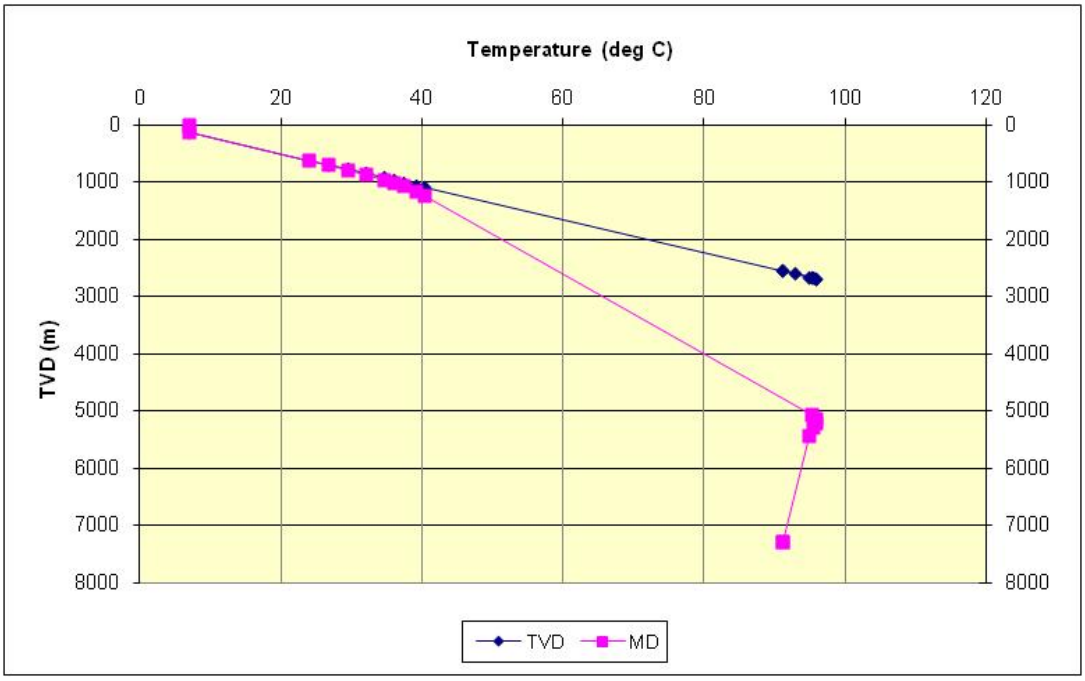

Figure 19 Geothermal gradient of S-02 well

The water temperature is assumed to be 7 degC and the reservoir temperature is 93 degC. The linear gradient temperature within true vertical depth is used in this thesis.

The gas lift data was input based on "the valve depth specified" type. Three gas lift valve positions were inputted in the model (1104, 2974, 4164 m, MD).

4.1.2 PROSPER Validation

Prosper model was matched to the actual model since the S-02 well was produced in March 2006. To ensure that vertical lift performance correlation used in this model was representative to the actual data, comparison between the calculation of the vertical lift performance and the actual measurement from the permanent downhole pressure gauge was performed. The following figure shows the result of the comparison. Petroleum expert 2 was used based on engineering judgment since Petroleum Expert 2 seems to be the similar to the model that used for the Petroleum Expert 2 calculation. In Prosper, the downhole gauge pressure is calculated by setting up the bottom hole pressure at the gauge depth. The menu of "calculate BHP from WHP" is used for the calculation.

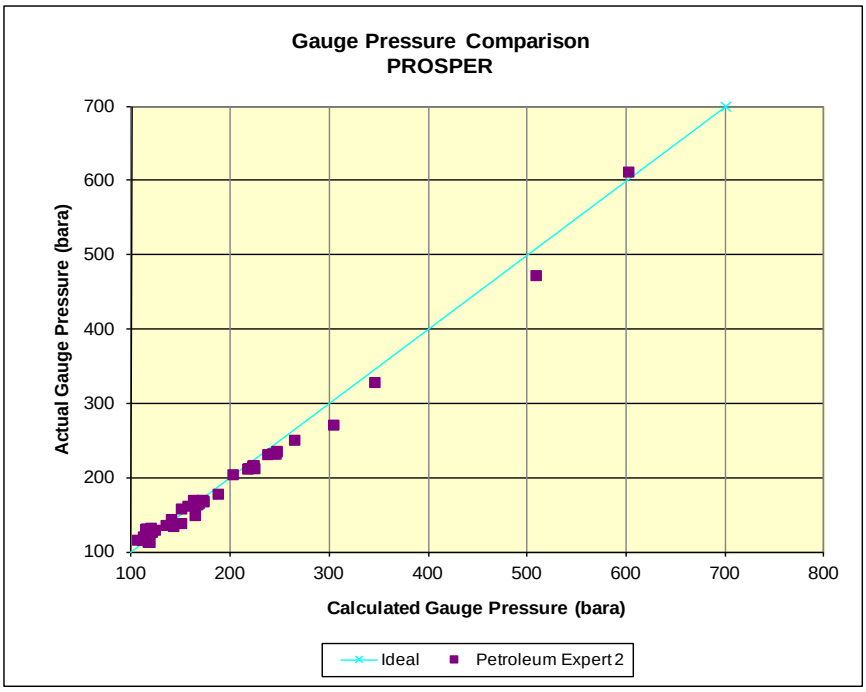

Figure 20 Vertical lift performance correlation validation to welltest data in Prosper

Figure above shows the result of using Petroleum Export 2 for the vertical lift performance of S-02 well. The calculated gauge pressure from Prosper looks match to the actual gauge pressure from the measurement. So, Petroleum Expert 2 will be used for the Prosper analysis in this thesis.

4.1.3 PROSPER Modeling Results

Gas lift design was performed in order to predict the best valve setting. Sensitivities of reservoir pressure, productivity index, GOR, water cut, and flowing tubing head pressure (FTHP) were done to analyze the design and the stability of the design. The following table shows six sensitivities based on the prediction from VIP simulator.

Table 2 Sensitivities of gas lift design in Prosper

No	Pres (bara)	PI (stb/d/psi)	GOR (scf/STB)	WC(%)	Max operating liftgas available (ksm3/d)	Max liftgas available during unloading (ksm3/d)	Max Liftgas supply pressure under operating conditions (barg)	Max Liftgas supply pressure at kickoff (barg)	Liftgas SG @ SC (20°C 1 bara)	Liftgas T (deg C)	FTHP (bara)
1	184	11	960	20,00	84,6	141,6	116	116	0,7	2	37,5
2	170	11	983	22,00	84,6	141,6	116	116	0,7	2	34,7
3	160	10	1022	24,30	84,6	141,6	116	116	0,7	2	33,7
4	153	9	1039	25,70	84,6	141,6	116	116	0,7	2	43
5	146	8,00	1067	27,50	84,6	141,6	116	116	0,7	2	40,5
6	125	5,00	1235	33,00	84,6	141,6	116	116	0,7	2	41

The sensitivities represent the well and reservoir condition within time. There will be decreasing of reservoir pressure, decreasing of PI, increasing of GOR, increasing of water cut and adjustment of the flowing tubing head pressure. However, the gas lift consumption and supplied pressure are kept at the same setting. The gas lift will be supplied from PH platform in the center of Valhall and will be allocated for S-02 well at around 141.6 ksm^3/d and 116 barg at the casing of S-02 well.

The following table shows the result of the gas lift design for S-02 well based on the calculation by PTC.

Table 3 Prosper result of gas lift design and stability criteria[23]

GLM	Valve Type	Port (1/64th)	P dome @18 C (bara)	GL Injection Rate (MMSCFD)
0	Unloading	10	105.2	0.5
1	Unloading	13	106.9	1
2	Orifice	19	n/a	3

In terms of stability, analysis of orifice valve selection is performed PTC with the comparison to the nozzle-venturi type (Stealth™ valve). Figure below shows the comparison between conventional orifice and the stealth orifice. Stealth orifice can reach critical gas lift rate at the higher tubing pressure based on the required gas lift rate. The orifice type of gas lift valve shows that the operating gas lift injection is below the critical rate. There is a risk of casing heading during the operation.

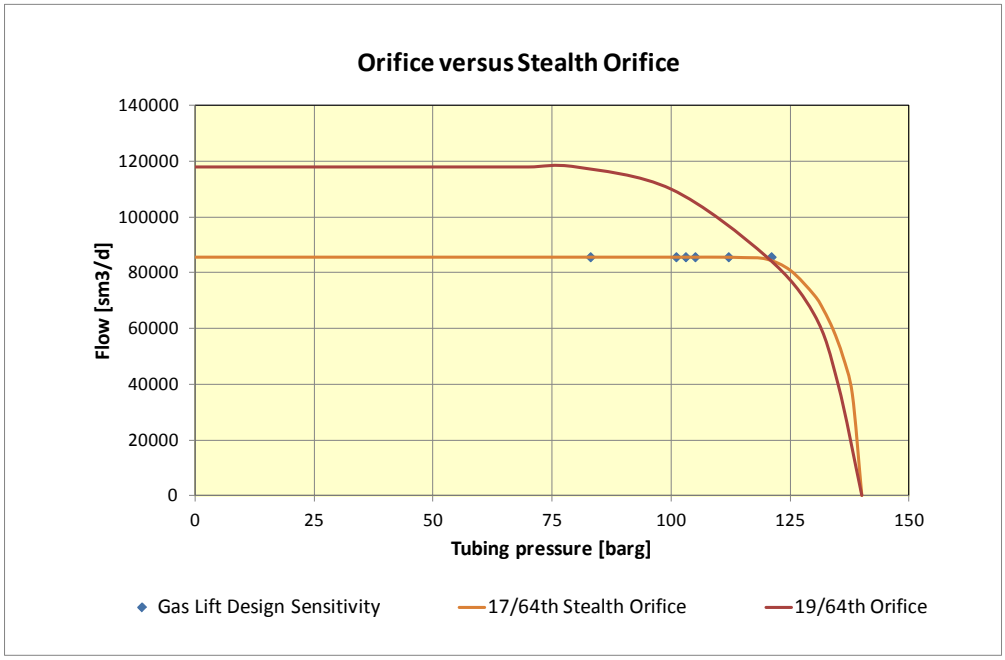

Figure 21 Conventional versus Stealth orifice in gas lift design[23]

4.2 OLGA MODELING

OLGA is used to model the dynamic behavior of S-02 well. OLGA predicts transient multiphase flow using a numerical method. The numerical calculation is based on the discretization and solution algorithm of repeated linearization (Newton-Raphson).In this study, the well module is used to simulate the transient multiphase flow in the wellbore. The model is validated by comparing downhole gauge pressure measurements to calculated pressure at the gauge depth. This process is done to ensure that the well model that is built is representative to the actual condition, especially to the vertical lift performance. Several sensitivities are performed to explain the effect of well geometry and to understand the behavior of gas lift operation in the complex well geometry.

The diagram below shows the detail steps of OLGA modeling including the validation and the sensitivities that are performed in this study.

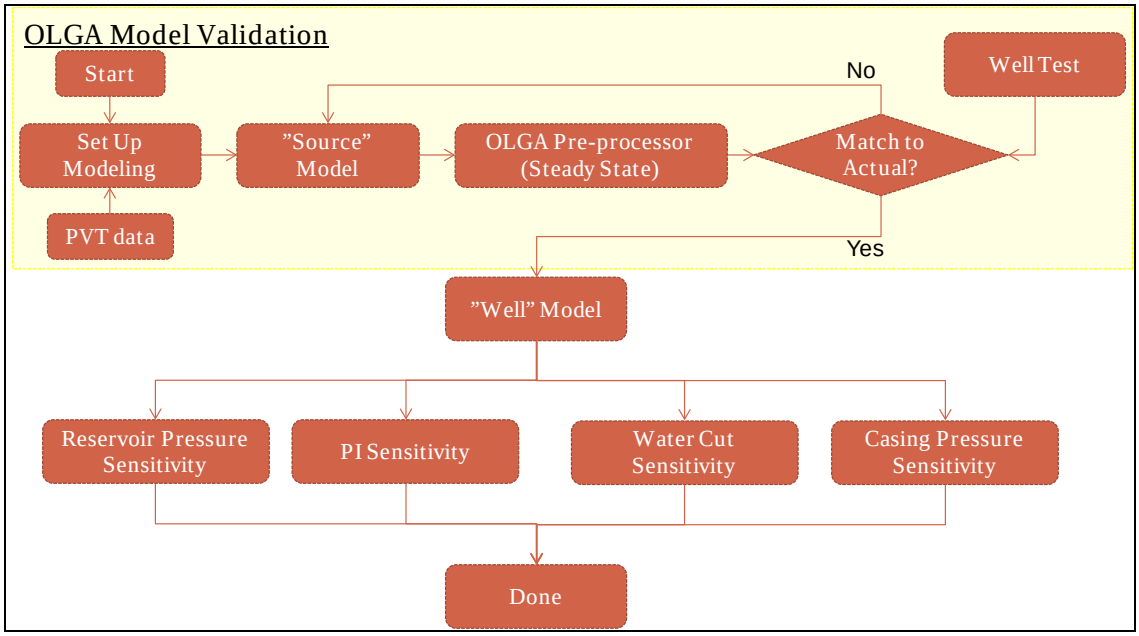

Figure 22 OLGA modeling

The modeling was started by creating PVT data in PVTsim. After setting up the model, the vertical lift performance correlation validation was performed to ensure that the model that used in this study is representative to the actual condition using OLGA pre-processor. After the validation, the transient model is used for several sensitivities to answer the objectives of this study. The details of the study will be explained in the following sub-chapters.

4.2.1 Developing The Models

4.2.1.1 PVT Data

The PVTsim is used to develop the PVT data that can be used in OLGA. There are two PVT data that are used in this model; PVT for reservoir fluid and PVT for the gas lift injection. The table below shows the base PVT description that used in this study for the reservoir fluid. However, the water cut and the GOR are inputted manually in OLGA to achieve an accurate match to the actual condition.

Table 4 The base PVT description used in the modeling

Component	Mol %	Mol wt	Liquid Density
N2	0.205	28.014	
CO2	0.205	44.01	
C1	45.704	16.043	
C2	5.169	30.07	
C3	3.132	44.097	
iC4	0.873	58.124	
nC4	3.285	58.124	
iC5	1.129	72.151	
nC5	1.54	72.151	
C6	2.874	86.178	663.9999
C7	1.89	96	767.1933
C8	1.792	107	776.1964
C9	1.7	121	784.1376
C10-C19	8.506	195.264	816.5793
C20-C27	5.289	322.745	848.7081
C28-C34	3.33	428.459	867.4054
C35-C40	3.841	519.876	880.2736
C41-C47	2.388	610.459	891.0263
C48-C55	2.44	714.978	901.6152
C56-C62	1.877	820.459	910.8209
C63-C71	1.57	931.432	919.3449
C63-C71	1.259	1057.432	927.8552

The following table shows the gas lift injection PVT based on the actual sampling. There are two kinds of PVT data that used in OLGA; black oil model and compositional model. In this study, most of the sensitivities uses black oil model. However, to ensure that two PVT data can be used, the standard conditions of both of them are similar.

Table 5 The PVT data of gas lift injection

Component	Mole %
Nitrogen	0.23
Carbondioxide	0.36
Methane	85.36
Ethane	9.53
Propane	3.73
i-Butane	0.21
n-Butane	0.51
i-Pentane	0.04
n-Pentane	0.03
Hexanes +	0
Total	100

4.2.1.2 Setting up the Model

The well is modeled based on the geometry of the well. The dynamic model is consisted of two geometry; well (tubing) geometry and annulus geometry. The diagram below shows the well diagram that used in OLGA.

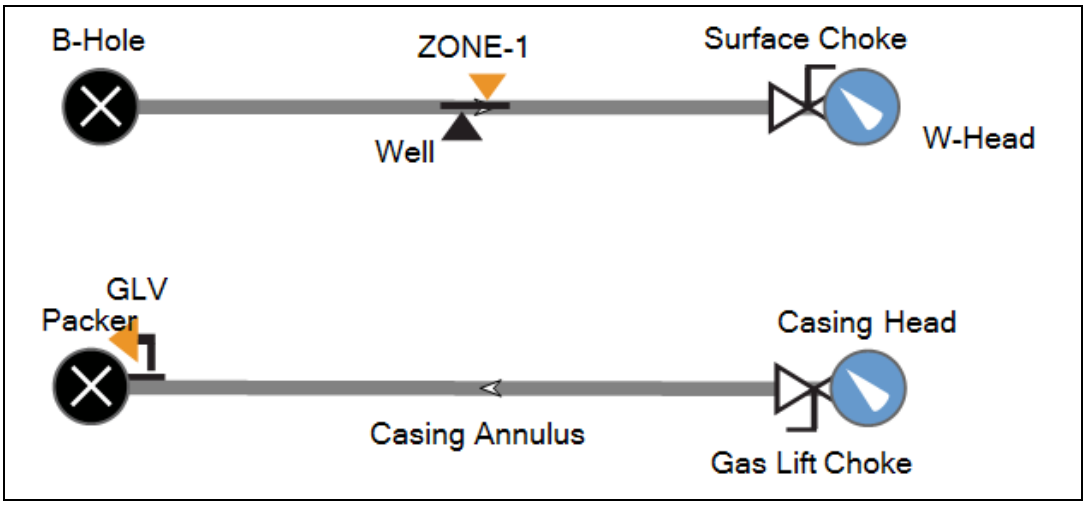

Figure 23 Well diagram in OLGA

The tubing performance was modeled from the "bottomhole" up to the "wellhead". The bottomhole was modeled using the closed boundary and the wellhead was modeled using the pressure boundary. The "Zone-1" was added to model the inflow performance relationship (IPR). The IPR of Productivity Index (PI) was used since the similar type of model was used in steady state modeling using Prosper. The produced fluid produced from the "Zone-1" up to wellhead.

The casing was modeled from the “casing head” down to the “packer”. The casing head was modeled using the pressure boundary and the packer was modeled using the closed boundary. The gas lift valve was modeled using well extended module of gas lift valve. The stealth orifice was modeled using the gas lift valve at the nearest size that available in the model. Since there is no available stealth orifice in the module, the model uses the database from the Valve Performance Clearinghouse (VPC^{TM}) using a demo valve.

4.2.1.3 Well Geometry

One of the objectives of this study is to analyze the effect of well geometry especially the J-shaped of the well. The well geometry is modeled in Geometry editor software that is tie in to OLGA. The well is divided into 176 segments with the several points of interest which are:

- Wellhead depth (0 m, MD)
- Gas lift mandrel #1 depth (1104 m, MD)
- Gas Lift mandrel #2 depth (2974 m, MD)
- Gas Lift Mandrel #3 depth (4164 m, MD)
- Gauge depth (4200 m, MD)
- Bottomhole depth (7231 m, MD)

The well geometry of the well is shown in Figure 24.

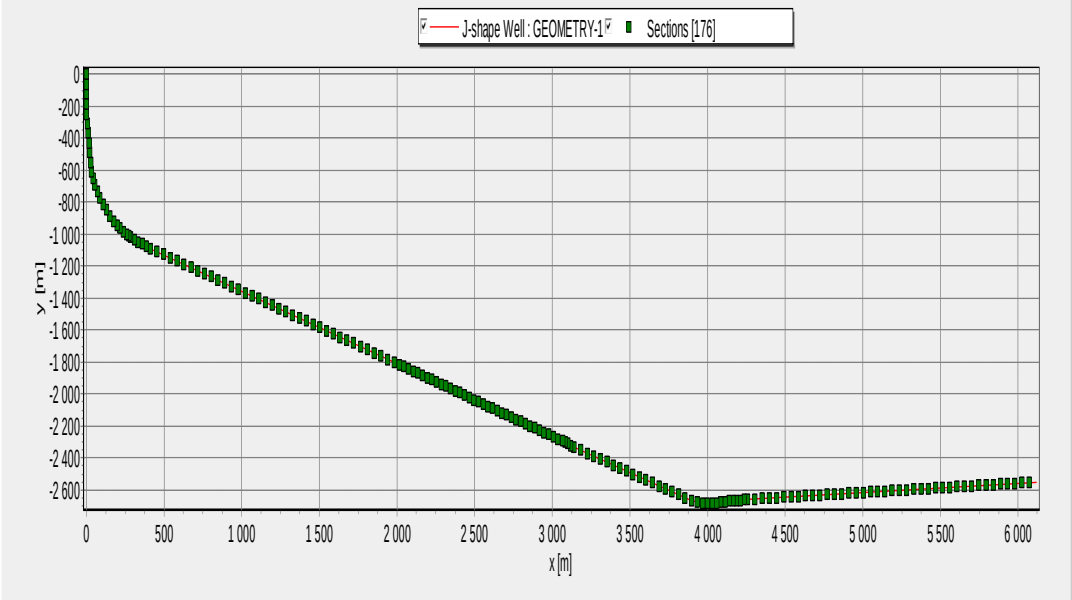

Figure 24 J-shaped well geometry

4.2.1.4 Model Validation

Validation in OLGA is performed by comparing the gauge pressure data from OLGA calculation and actual data from gauge measurement. There are 47 well test data since

March 2006 until November 2011 that are used for this validation. The figure 21 shows the steps to do the validation. The well in OLGA is modeled by using the "source" model where the certain fluid is produced from the reservoir. OLGA is used to calculate the gauge pressure data based on the other input using well test data. The comparison of gauge pressure data between the OLGA calculation and the actual measurement from the gauge is used to validate the model.

The figure below shows the comparison between the actual measurement from the gauge data and the OLGA calculation. From the figure, it can be seen that the gauge pressure calculated and the actual measurement from the gauge are relatively matched. The data are distributed close to the ideal line where the actual gauge measurement is the same as the OLGA calculation. From this comparison, it can be concluded that the OLGA modeling can be used for analysis.

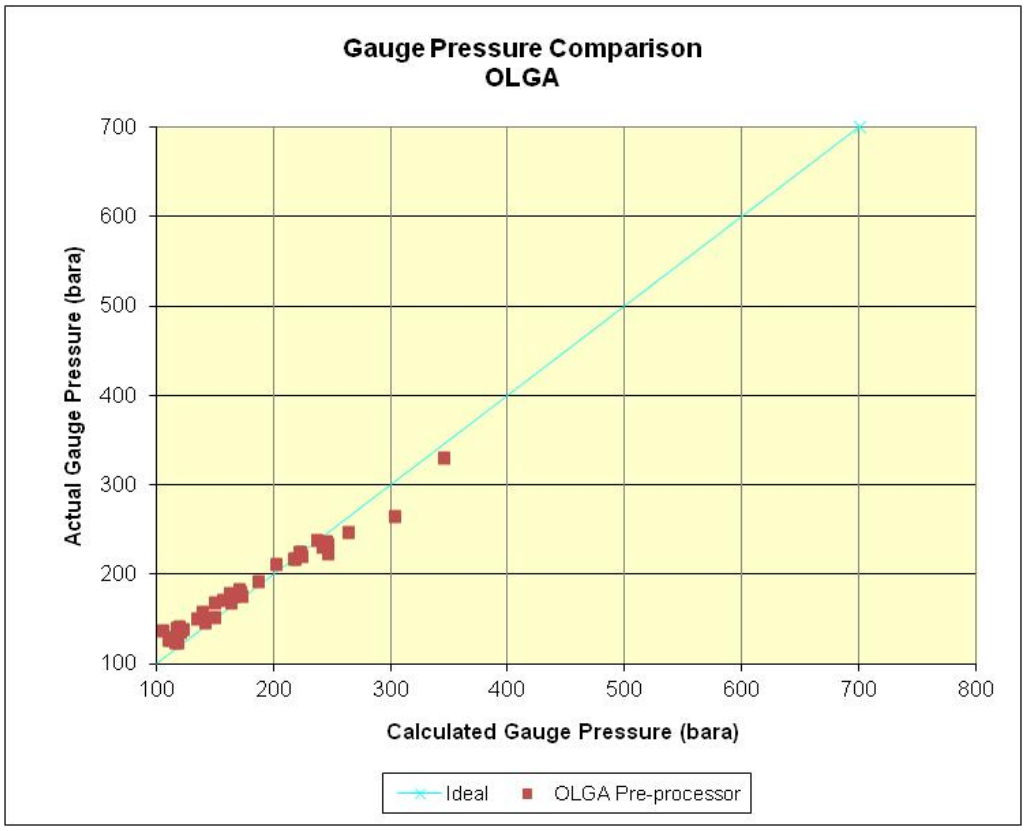

Figure 25 Vertical lift performance correlation validation to welltest data in OLGA

4.2.2 Startup Procedure

In order to simulate more reliable startup and unloading behavior, shut in and start up procedure is modeled is OLGA. Three periods is simulated. The first period is where the well is produced in the first 3 hours to be able to simulate steady state behavior. This period

models the steady state behavior as a preparation for well to be shut in. The second period is where the well is shut in the next 3 hours to allow the fluids to segregate by closing the surface choke in the wellhead. The third period is where the well is produced for another 9 hours to simulate the startup and the steady state behavior. Figure below shows the surface choke opening profile over time as a description of the three periods. When the well is produced, the surface choke is fully opened. However, the stroke time of valve opening (opening the well gradually) is added in some cases to ensure that the well is not numerically error because of the Joule-Thompson effect.

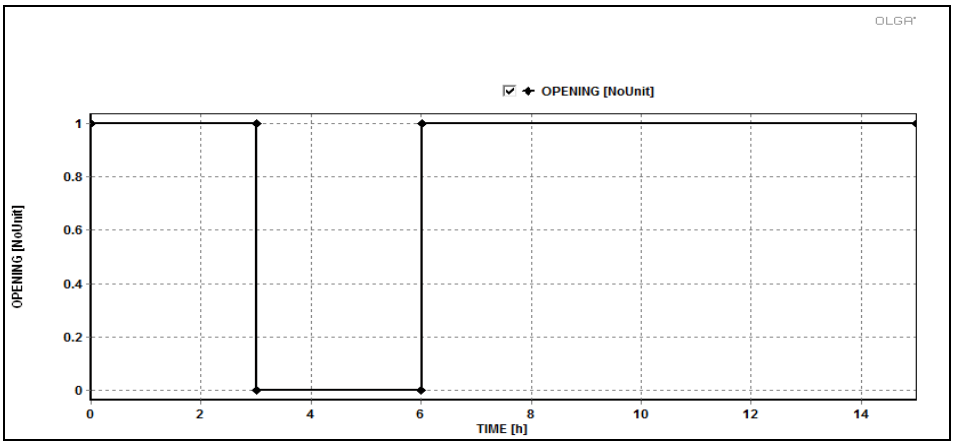

Figure 26 Opening sequence for all cases

4.2.3 Use the Models

There are five cases that are used in this study to evaluate the vertical lift performance in a complex gas lift well geometry. There are four sensitivities that performed for each case which are reservoir pressure, productivity index, water cut, and casing head pressure. The detail of each case will be explained in the following section.

4.2.3.1 Case #1 J-Shaped Well (Base Case)

Case #1 models the condition where S-02 is produced naturally. The objective of this case is to understand the behavior of the J-shaped vertical lift performance in natural flowing well. Several sensitivities are performed in order to understand the effect of complex well geometry of J-shaped well; reservoir pressure, productivity index, and water cut.

Well and Startup Performance

The figure below shows the behavior of the well at 15 hours of production when the well is relatively in stable condition. The figure shows the behavior of the well along the depth. The pipeline length of 0 m represents the bottomhole of the well and the

pipeline length of 7301 m represents the measured depth at the wellhead. OLGA shows the well distribution result from upstream to downstream where bottomhole is the upstream and the wellhead is the downstream. The oil production is around 7000 b/d and the gas production is around 7 MMscfd.

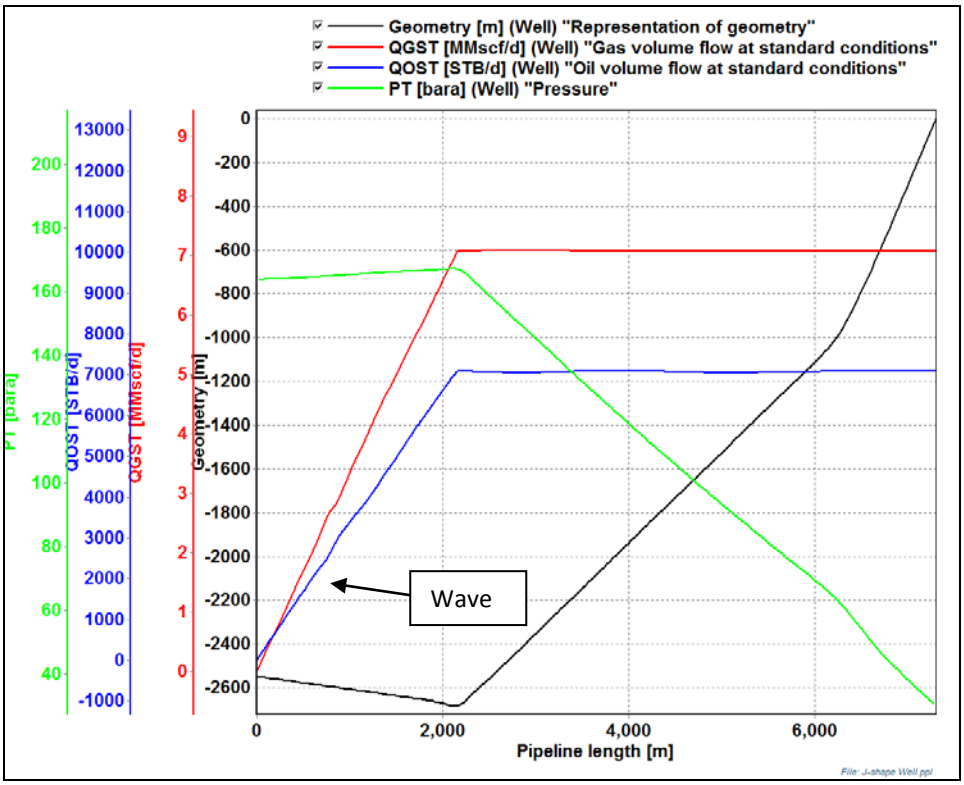

Figure 27 Well behavior of J-shaped well

The bottomhole pressure is between 160-170 bara. It shows that the well needs around 40-50 bar of drawdown to produce the fluid. The J-shaped well creates unique pressure distribution along the well. The pressure increases until the deepest true vertical depth of the well (at 2681.78 m, TVD) which is around 161.5 bara and decreases to 30 bara at the wellhead. The fluids are produced from the distributed reservoir section along the J-section from the toe to the heel of the section. It is observed some waves in the production rate from the reservoir section.

The analysis of well behavior during startup is also performed in order to understand the effect of well geometry to well startup performance. The detail analysis of production rate, pressure, and holdup are monitored during the well startup.

The definition of well startup in this study is after 3 hours of shut in. The bottomhole pressure behavior is assumed to be stable after 3 hours of shut in. Based on the

figure, the analysis of startup performance is started at time is equal to 6 hrs and end when all parameter has been in stable condition.

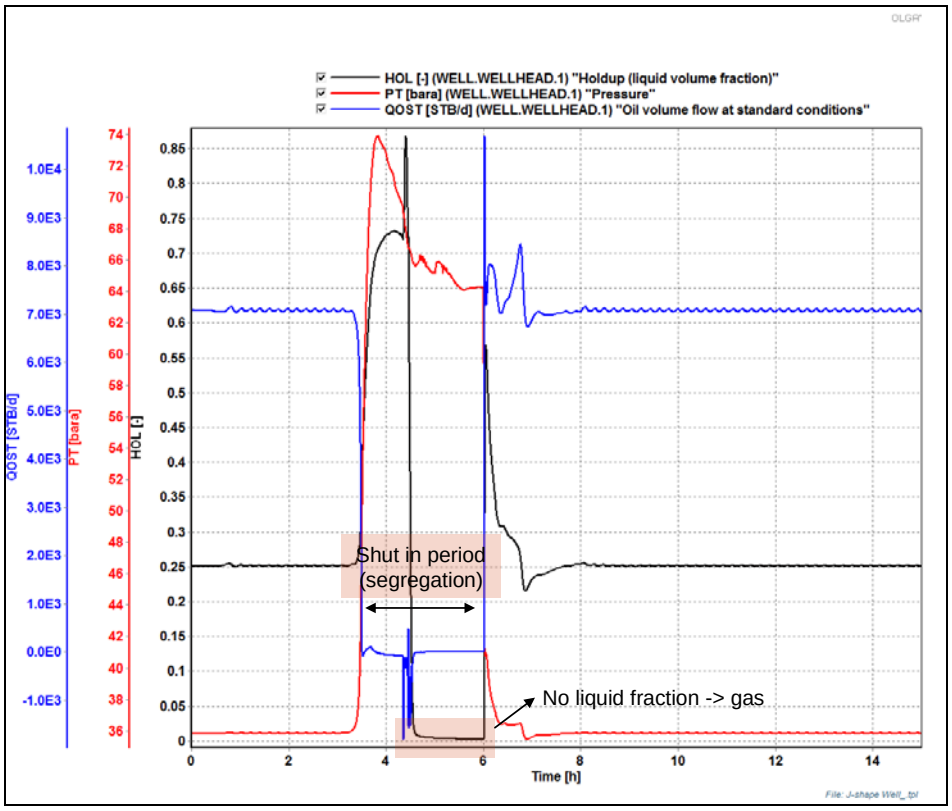

Figure 28 Wellhead behavior

The figure above shows the wellhead behavior over time. Oscillation amplitude is observed during steady state behavior. During the shut in, the wellhead increases for about 28 bara from 36 bar up to 64 bara. Figure 28 Wellhead behavior is compared to Figure 29 Gauge depth behavior.

The fluids are segregated. The liquid is accumulated at the bottom part of the well shown by the holdup is equal to one at the gauge depth section. The gas is accumulated at the upper part of the well shown by the holdup equal to zero at the wellhead section. When the well is opened, some fluctuations are observed called by static instability. The equilibrium is reached when the wavy flow (oscillation) is observed during the steady state condition. It has prone to slugging.

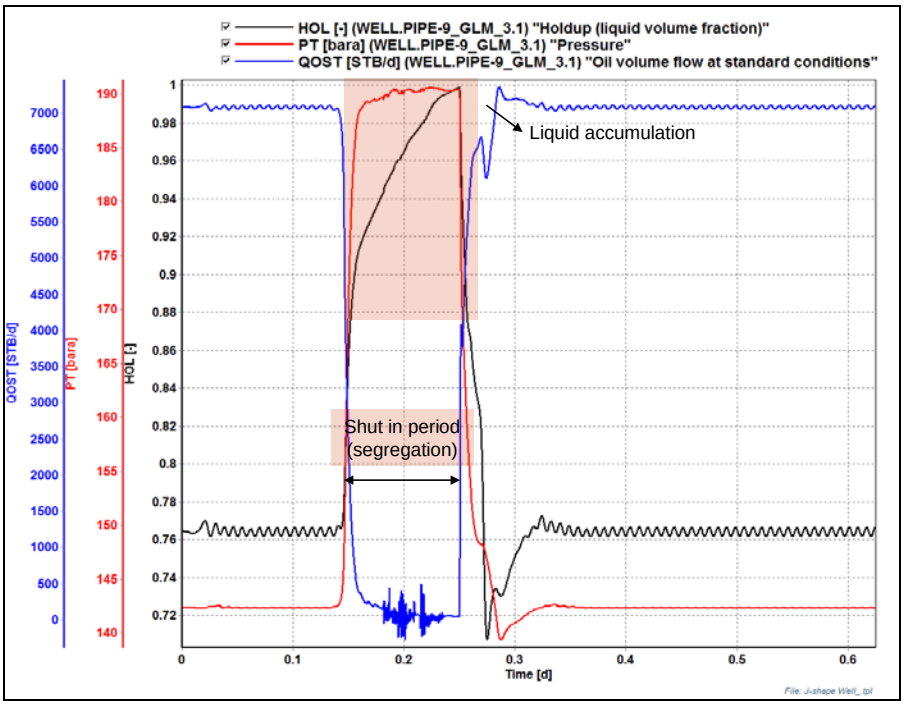

Figure 29 Gauge depth behavior

Figure 30 shows the three dimension of holdup along the well at different time. At t_1, the well is shut in. The fluids are segregated based on the density. At t_2, the well is opened and the well head pressure decreases. The drawdown is established in the bottomhole. The bottomhole pressure is below the bubble point so that the gas is dissolved from the oil. The gas dissolved is accumulated at the toe section of the J-shaped well. The different superficial velocity between the gas and liquid establishes a wavy flow arising from gas blowing over the surface and has prone to slugging.

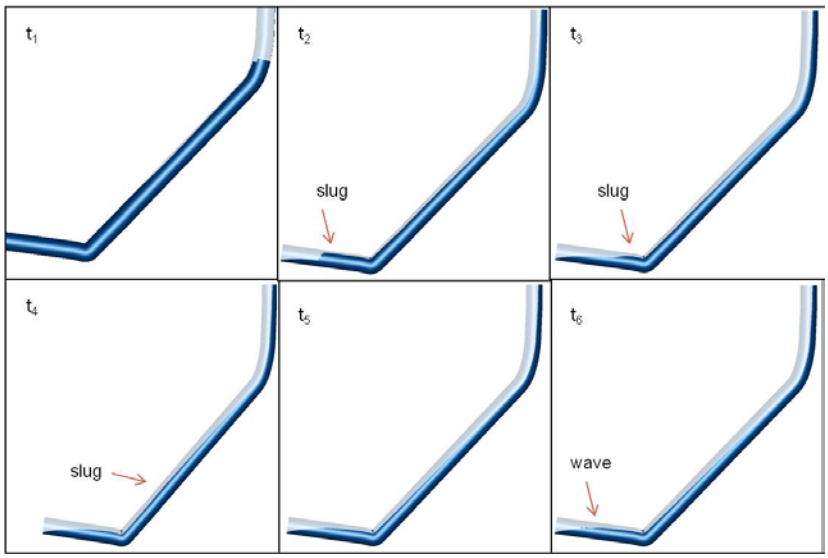

Figure 30 Holdup behavior for J-shaped well

At time t_3, the slug flows in the J-section of the well. The fluids are segregated along the downward incline section of the well during flowing. Dissolved gas is produced from the toe of the J-section. Most liquid is produced from the heel of the J-section. At time t_4, the slug flows in the middle of the upward incline section. At time t_5, a stable flow is reached. However, time t_6 shows that wave is initiated when the steady state condition is reached.

A failed startup well is also analyzed in this study. From Figure 31, the well is not able to be online when the reservoir pressure is below 180 bara. The detail analysis at this pressure is performed during the startup of the well. The holdup behavior of the well is shown in the below figure.

When the well is shut in (t_1), the fluids are segregated based on the density. The liquid phase is accumulated in the bottom part where the gas phase is accumulated on the top of the well. When the surface choke is opened (t_2), the well is flowing. The wellhead pressure decreases. A drawdown is established in the bottomhole. A dissolved gas is observed in the bottomhole.

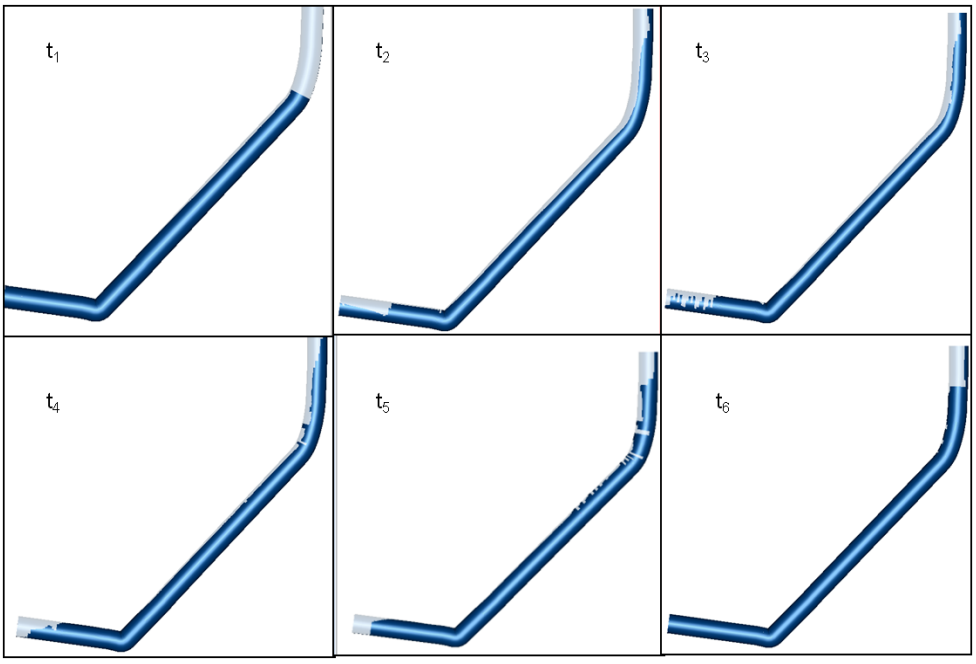

Figure 31 Holdup behavior of failed startup

At time t_3, the fluids are segregated and the hydrostatic head increases. The higher hydrostatic head initiates the higher bottomhole pressure and lower drawdown. Time t_4 shows the fluid is accumulated along the well and the increase of bottomhole pressure decreases the volume of the dissolved gas. Time t_6 shows that

the well is not able to be produced when the bottomhole pressure is the same as the reservoir pressure. No drawdown is established in the bottomhole. The fluid is accumulated in the bottom part of the well and the gas is accumulated on the upper part of the well. The well is in static condition.

Well Sensitivities

The reservoir pressure sensitivity is performed to analyze the effect of different reservoir pressure to the well performance that shown in Figure 32. Five cases of different reservoir pressure (210, 200, 190, 180, 170 bara) are analyzed. The oscillation (wave) of production rate is also observed in this figure. The steady state calculation shows that the well can be produced for all sensitivities of reservoir pressure. However, when the well is shut in, it is difficult to startup the well especially at low reservoir pressure (below 190 bara). The segregation of the fluids during shut in creates startup problem in the low reservoir pressure wells. In order to evaluate the possibility of producing well without the aid of gas lift, segregation simulation during shut in and startup/unloading sequence are needed to be modeled.

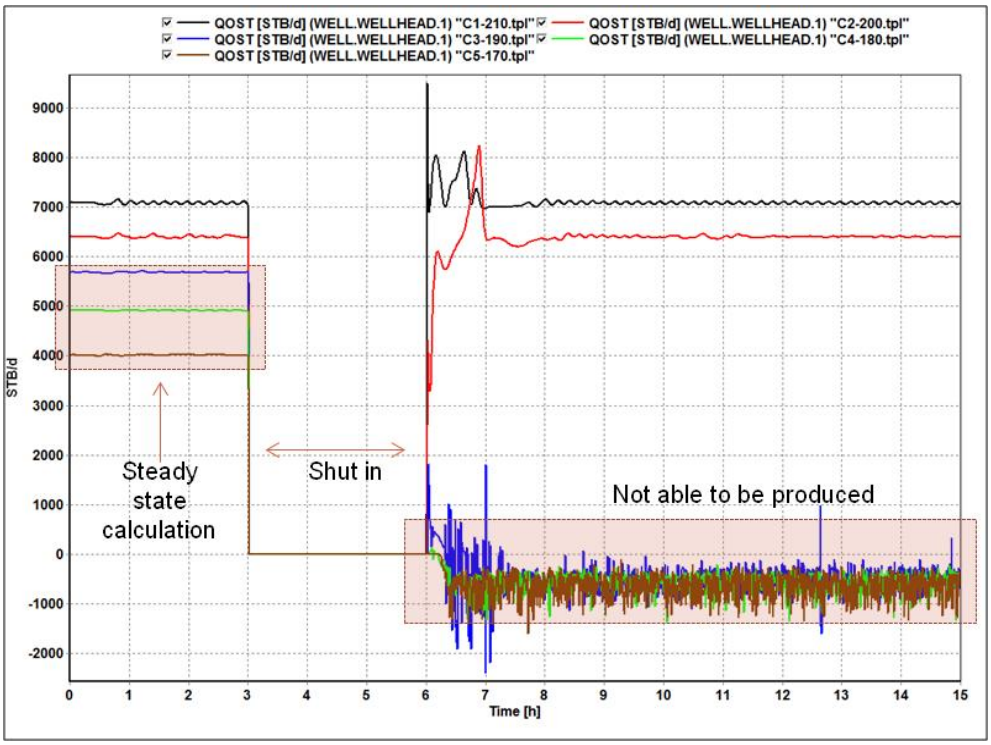

Figure 32 Reservoir pressure sensitivity for J-shaped well

The productivity index sensitivities are performed to see the effect of different productivity index to the well performance that shown in Figure 33. Three cases of different productivity index (11, 9, 5 STB/d/psi) are analyzed.

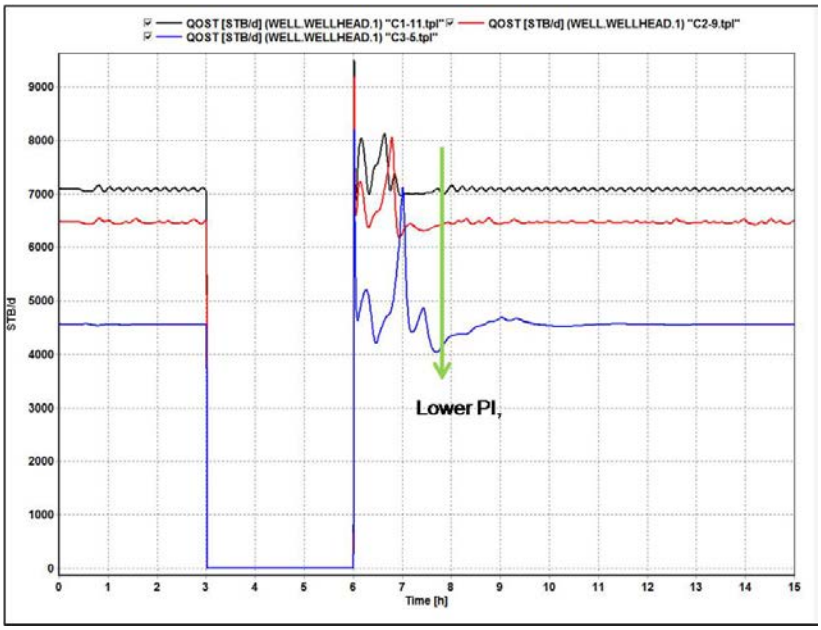

Figure 33 Productivity index sensitivity for J-shaped well

From the result, the well can be produced even at lower productivity index. However, more fluctuation during the startup is observed for the well with lower productivity index.

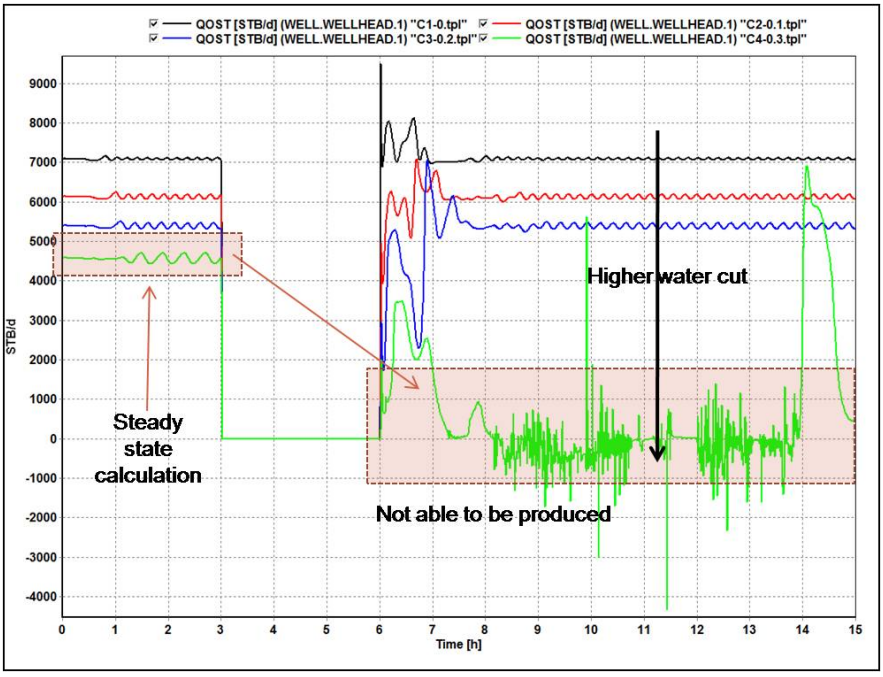

Figure 34 Water cut sensitivity for J-shaped well

The water cut sensitivities are also performed to analyze the effect of different water cut to the well performance. Four sensitivities of different water cut (0, 0.1, 0.2, and 0.3) are analyzed that shown in Figure 34. Oscillation amplitude increases as the water cut increases. When the water cut is higher than 0.3, it is difficult to startup the well. The steady state calculation shows that the well can be produced. However, the segregation of the fluid during shut in period introduces a difficulty of well startup, especially in the higher water cut. In terms of dynamic instability, the oscillation amplitude increases when the water cut increases.

4.2.3.2 Case #2 Horizontal Well

Case #2 models the horizontal section instead of J-shaped section in the bottomhole. The objective of this case is to analyze the effect of well geometry to the well performance. Hypothetic well is built for the horizontal well using a typical well geometry based on the S-02 well. The horizontal section is started at the depth of 4988 m, MD where the well reaches the middle true vertical depth of the reservoir section. From the depth of 4988 to 7301 m, MD, the well is configured as a horizontal section.

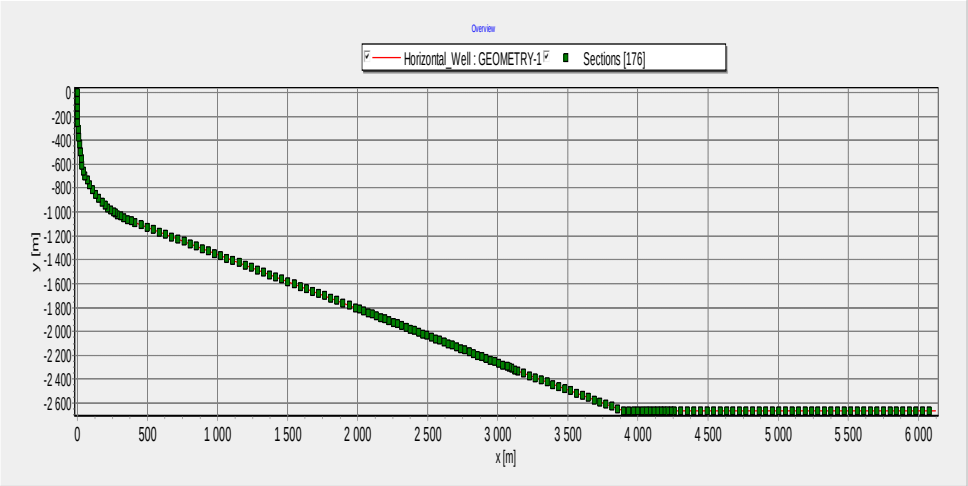

Figure 35 Horizontal well geometry

Well and Startup Performance

The figure above shows the well configuration for this case. The different of well geometry can be seen by comparing Figure 17 and Figure 35 as shown as Figure 44. Figure 17 shows the J-shaped well geometry based on the actual well geometry of S-02.

Figure 35 shows the hypothetic well geometry that created for this study. Figure 36 shows the behavior of the oil production for J-shaped and horizontal well. Both of them are produced at the relatively similar oil rate. However, the J-shaped well shows unstable behavior (oscillation) compared to the horizontal well. The well behavior at different position (gauge depth and wellhead) is analyzed.

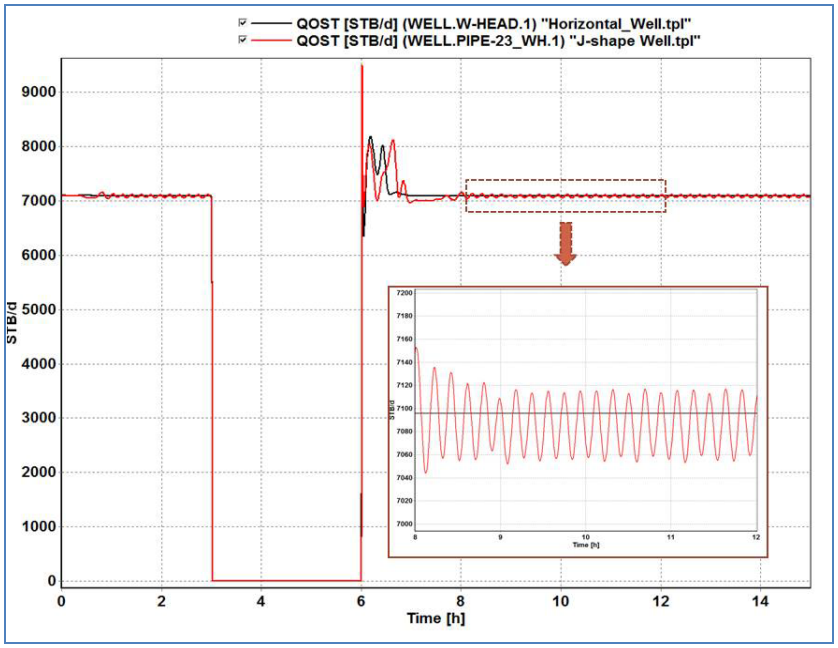

Figure 36 Oil rate behavior for J-shaped (red) and horizontal (black)well

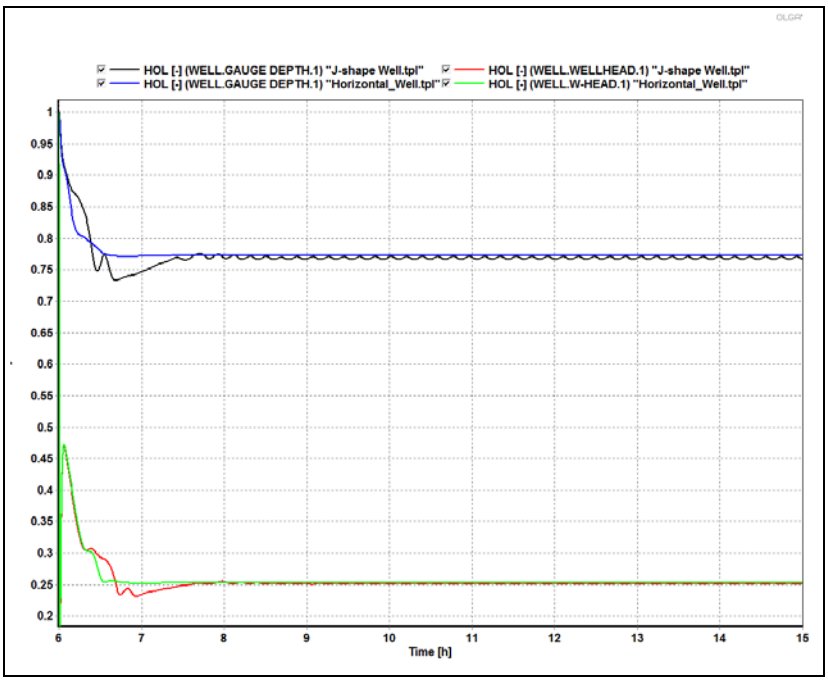

Figure 37 Holdup behavior for J-shaped (black & red) and horizontal well (blue & green) at two different position

Figure 37 shows the comparison of holdup behavior between the J-shaped and the horizontal well.The black line is the holdup behavior of J-shaped well at the gauge depth while the blue line is for the horizontal well. The red line is the holdup behavior of J-shaped well at the wellhead depth while the blue line is for the horizontal well. The relatively higher holdup at the gauge depth position than the wellhead position shows the distribution of the liquid along the well during production. During production, it is observed that the holdup is distributed from higher holdup in the bottom part of the well to the lower holdup in the upper part of the well.

Figure 38 shows superficial oil and gas velocity, holdup, and geometry for the J-shaped and horizontal well. The holdup of J-shaped well is shown by the light blue line while the horizontal well is shown by the light green color. A wave is observed in the certain depth of the reservoir section in the holdup of J-shaped well but not for the horizontal well. The holdup also shows segregation at the tip of the J-section (from toe to heel). Gas is accumulated at the toe while the liquid is accumulated at the heel.

Superficial oil velocity for the J-shaped well is shown by the light brown line while the horizontal well is in dark blue line. Superficial gas velocity for the J-shaped well is shown by the pink line while the horizontal well is in red line. Both superficial oil and gas velocity shows relatively similar trends along the well. At the heel of both wells, the low velocities are observed. Some liquid tends to collect in the low points of the well.

The downward inclination of the J-shaped well introduces periodic waves over time arising from gas blowing over the surface. This introduces periodic fluctuation of the superficial gas and liquid velocity in the J-shaped well.

Change of superficial velocity is also observed when the inside diameter (ID) of the well changes. The larger inside diameter introduces lower velocity. This behavior is observed in both superficial gas and oil velocity in the J-shape and the horizontal well.

From the analysis above, the J-shaped well demonstrates unfavorable behavior compare to horizontal well. The J-shaped well is prone to slugging.

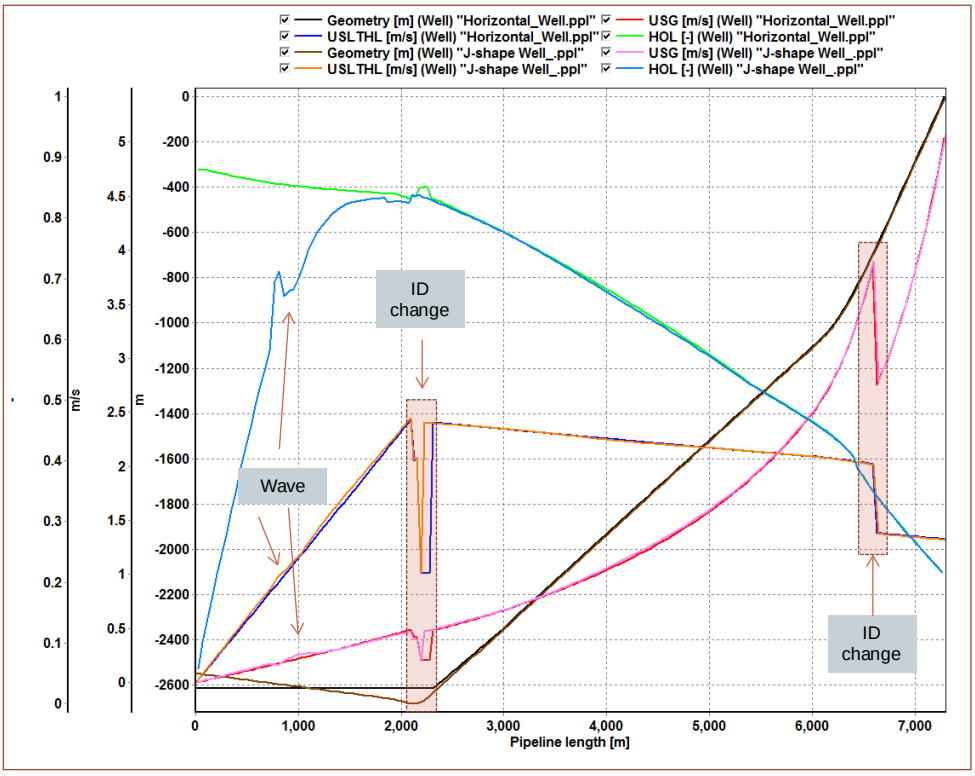

Figure 38 Oil and gas velocity, holdup and geometry of J-shaped (solid) and horizontal (dot) well

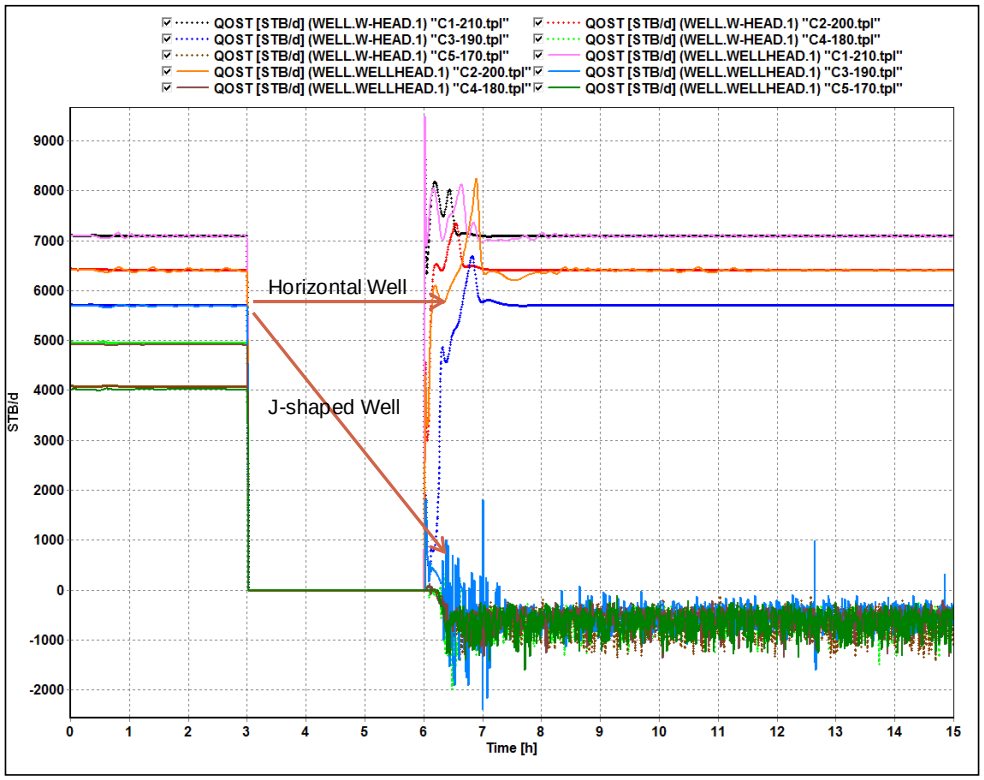

Figure 39 Reservoir pressure sensitivity for J-shaped (solid) and horizontal (dot) well

Well Sensitivities

Reservoir pressure sensitivity is also analyzed in this study. Figure above shows the well behavior at different reservoir pressure (210, 200, 190, 180, and 170 bara) for J-shaped and horizontal well. The dot line plots represent the horizontal well and the solid line plots represent the J-shaped well. The result shows that the horizontal well can be produced at lower reservoir pressure than the J-shaped well. At reservoir pressure of 190 bara, it is difficult to startup the J-shaped well. The steady state calculation shows that the well can be produced at lower reservoir pressure (190, 180, 170 bara). However, when the well is shut in, it is difficult to back online the well since the fluid has been segregated in the wellbore. The declining of the reservoir pressure introduces well startup problem in both wells. However, it is observed that the startup problem in the J-shaped well happened in the higher reservoir pressure than the horizontal well.

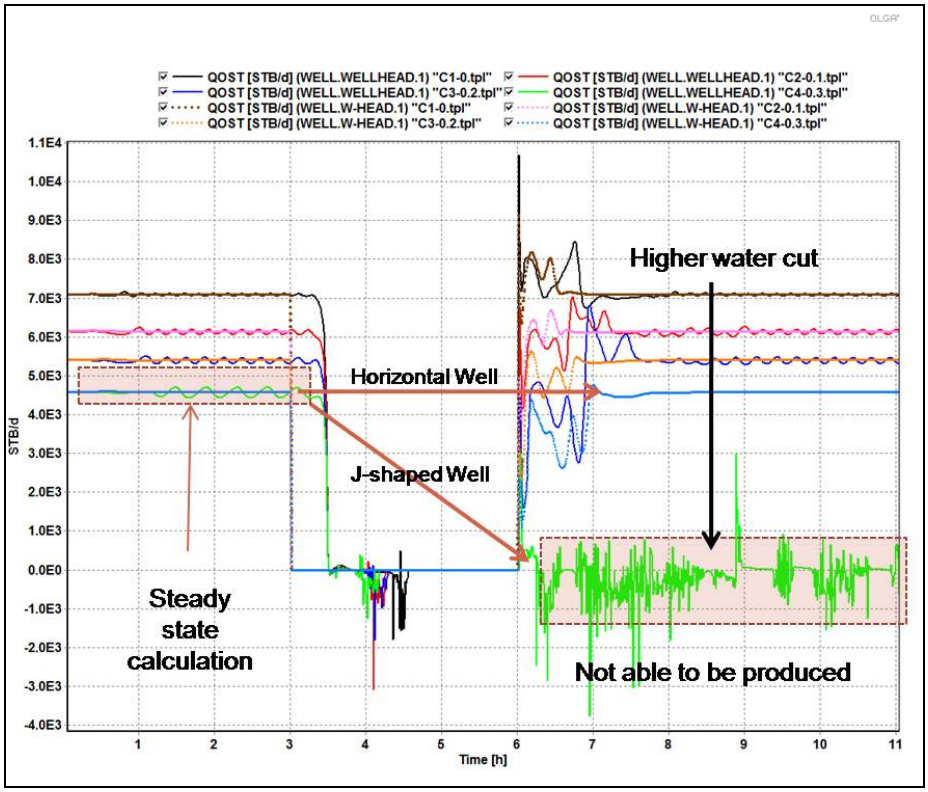

Figure 40 Water cut sensitivity for J-shaped (solid) and horizontal (dot) well

Water cut sensitivity is analyzed in this study. Figure above shows the well behavior at different water cut (0, 0.1, 0.2, and 0.3) for J-shaped and horizontal well. The dot line plots represent the horizontal well and the solid line plots represent the J-shaped well. The result shows that the horizontal well can be produced at higher

water cut than the J-shaped well. At water cut of 0.3, it is difficult to startup the J-shaped well. The steady state calculation shows that the well can be produced at high water cut (0.3). However, when the well is shut in, it is difficult to back online the well since the fluid has been segregated in the wellbore. The water production introduces well startup problem in both wells. However, it is observed that the startup problem in the J-shaped well happened in the lower water cut than the horizontal well.

4.2.3.3 Case #3 Transient Reservoir Behavior

Chapter 3 shows that the S-02 well has a strong transient behavior from the reservoir. This can be seen from the decline of bottomhole pressure and after 20 days of production, the well did not show any indication of reaching the steady state behavior. Case #3 models a decreasing of reservoir pressure to represent the strong transient behavior of the reservoir. 10 bar decreasing of reservoir pressure in the first three days and 1 bar reservoir pressure decrease in the last day of production are selected based on the actual observation of S-02 well. 24 days of simulation is used to mimic the actual condition. Case #3 models the inflow performance relationship using "well" component to be able to model the decreasing of reservoir pressure.

Table 6 Time series of reservoir pressure

Time (Days)	0	1	2	10	24
Reservoir Pressure (bara)	200	190	180	170	160

The table shows the time series of changing reservoir pressure. The transient reservoir behavior is analyzed as an effect of decreasing reservoir pressure.

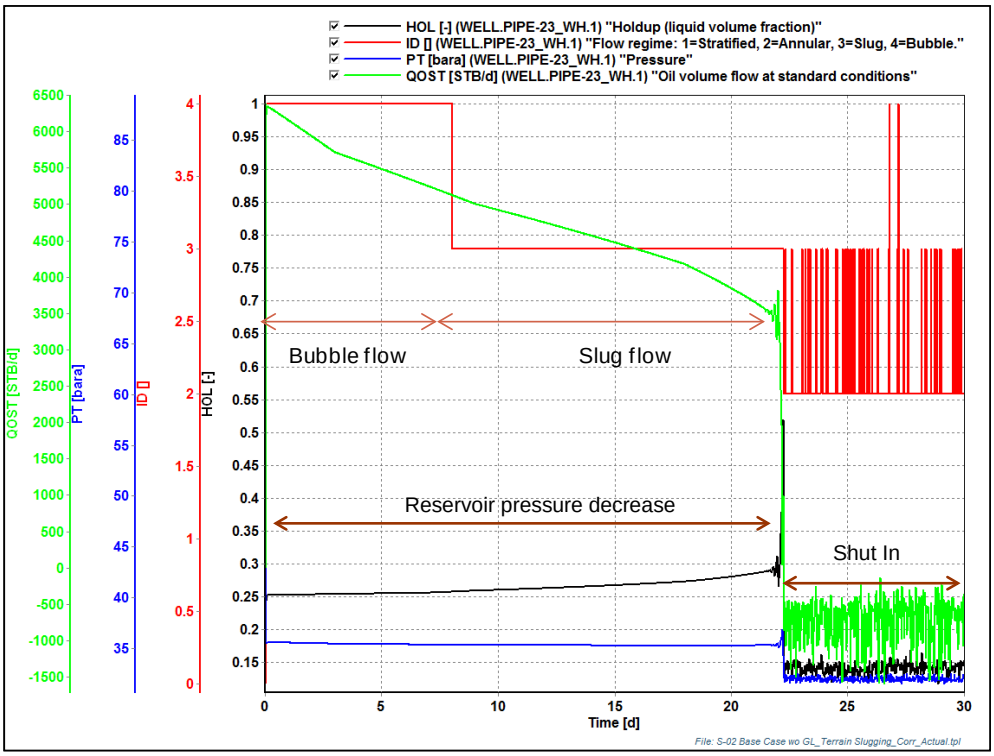

Figure 41 Transient reservoir behavior at wellhead position

This case shows that the well can be produced naturally until certain average reservoir pressure. In this case, when the well reaches around 160 bar of average reservoir pressure, the reservoir pressure is no longer able to create enough drawdown to overcome the pressure drop due to gravity and friction.

Figure 41 shows the transient behavior at the wellhead point. At the lower reservoir pressure, the risk of slugging is increasing. It can be seen from the flow regime behavior. When the reservoir pressure is going down, the well tends to create slugs. At the reservoir pressure at around 200 bara – 180 bara, the flow regime of the wellhead is still bubble. At the reservoir pressure lower than 180 bara, the flow regime changes to slug behavior.

Figure 42 shows the transient behavior at the gauge depth position. At the gauge depth, the flow regime of the well tends to be dispersed bubble along the time. It means that the liquid fraction is dominant in the bottom part of the well. The comparison between Figure 41 and Figure 42 also shows that certain depth establishes the transition of flow regime from bubbles to slug flow. The lower pressure in the shallower true vertical depth establishes more dissolved gas to the system. The bubble is then accumulated to create slug (Taylor) bubbles.

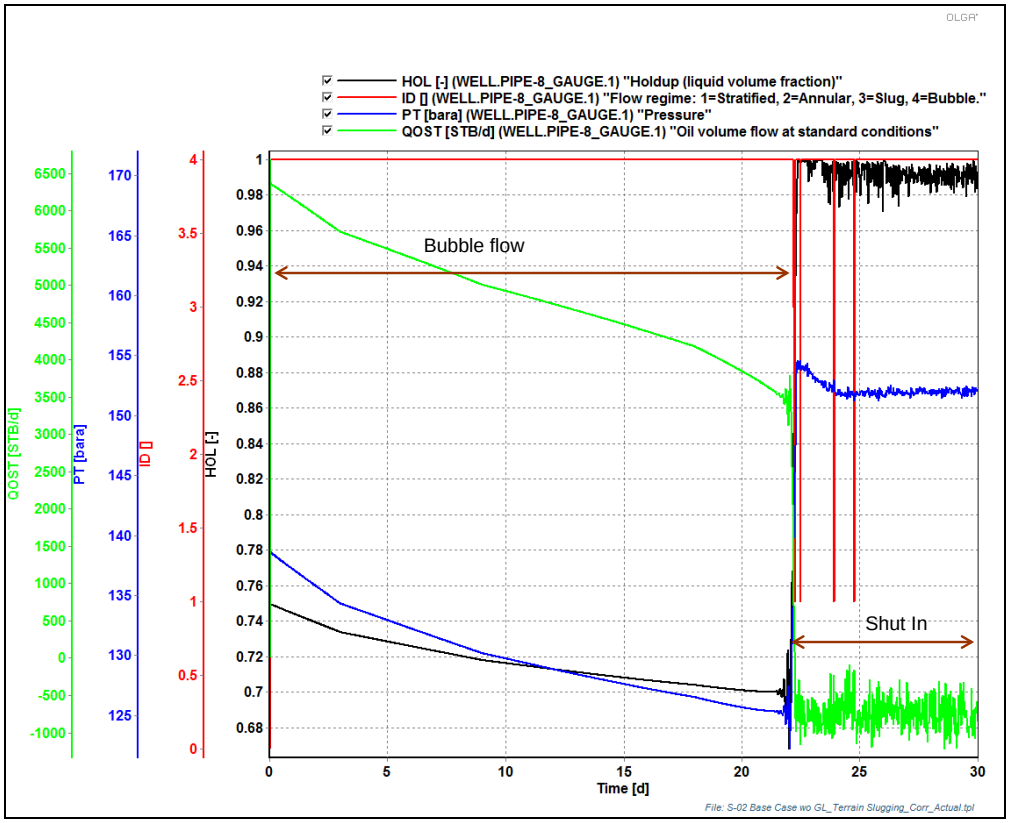

Figure 42 Transient behavior at the gauge depth position

When the well starts dying, rapid decrease of well production and increase pressure gauge behavior shows an agreement with the liquid hold up behavior. At this period, the fluids are segregated. The bottomhole pressure is similar to the pressure loss due to gravity and friction. The liquid is accumulated in the bottom part of the well and the gas is accumulated in the upper part of the well as shown as the holdup behavior along the well

Decreasing reservoir pressure at the near well bore area causes S-02 well to be produced in the cyclical basis. When the well is online, the decreasing reservoir pressure at the near wellbore area creates lower holdup in the wellbore. The decreasing reservoir pressure can not balance the increasing hydrostatic head along the wellbore and as a result, the well is shut in. During shut in period, the reservoir pressure at the near wellbore area increases until it reaches a certain pressure where the well can be produced again.

Case #3 confirms the result from case #1. In case #3, the simulation shows that the well can be produced until the reservoir pressure of 170 bara. Case #1 is also shown the same result. However, the required reservoir pressure during well startup is at

least 200 bara. This happened since the shut in condition leads to segregation of the fluid along the well and accumulation of liquid in the bottom part of the well. The fluid accumulation in the shut in condition leads to higher hydrostatic head compared to the flowing condition.

4.2.3.4 Case #4 J-Shaped Well with Gas Lift

Case #4 models the effect of gas lift to the vertical lift and the well performance. In this case, the gas lift is injected at the lowest gas lift mandrel (4164 m, MD). The port size of the gas lift valve in the model is 20/64th inch as the closest available port size that available in the OLGA demo database. The analysis of the well is modeled at the surface casing pressure of 120 barg which is based on the actual available gas lift pressure at the gas lift manifold in South Flank platform. The unloading valve is not modeled in this study.

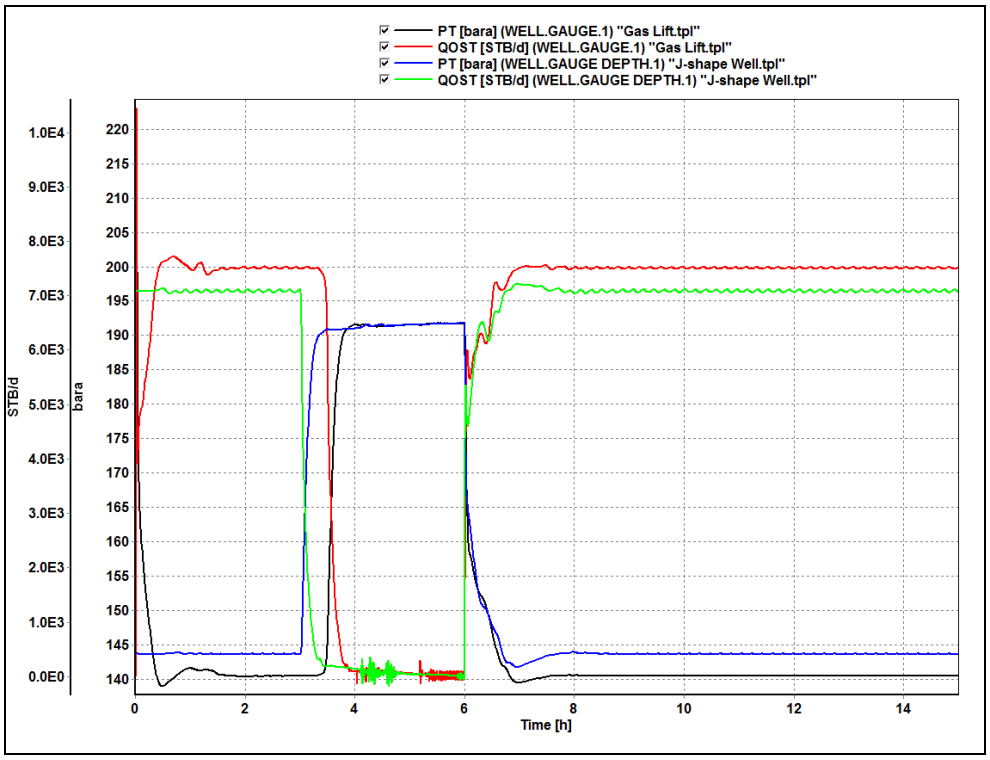

Figure 43 Well behavior at the gauge position for with and without gas lift well

Well and Startup Performance

Figure 43 shows oil production and pressure behavior at the gauge depth for the J-shaped well with and without gas lift. There is a small increase of the oil production when the gas lift is injected. The lower gauge pressure is observed when the gas lift is injected at the third mandrel at the same wellhead pressure. In the actual condition, higher wellhead pressure is observed at the similar gauge pressure (see Figure 11). In terms of startup performance, the well that is produced naturally (Case #1) is compared to the well that is produced with gas lift (Case #4). The figure below shows the comparison of startup behavior of the two cases.

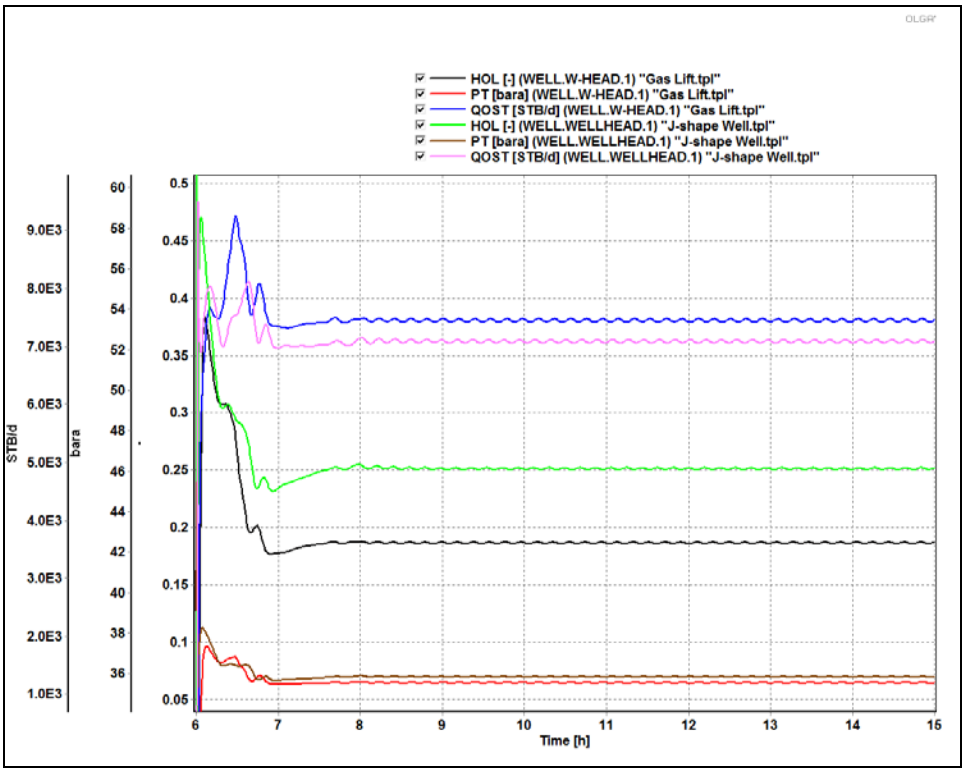

Figure 44 Start up behavior at the wellhead for with and without gas lift well

The blue line is the oil rate of the well using gas lift while the pink line is the oil rate of the well when it produced naturally. The red line is the wellhead pressure trend of the well using gas lift while the brown is the pressure of the well when it produced naturally. The black line is the liquid fraction of the well using gas lift while the green line is the liquid fraction of the well when it produced naturally.

The gas lift well produces at higher rates than the natural flowing well. However, it is not too significant. The gas lift establishes a lower bottomhole pressure. The drawdown increases so that the oil production of the gas lift well increases. In terms

of startup behavior, these two cases show relatively similar behavior. It shows that the gas lift establishes more fluctuation than the natural flowing well. The holdup of the gas lift well decreases in the wellhead as an introduction of more gas lift in the system. The wellhead pressure increases as a gas lift injected. The gas lift decreases the hydrostatic head above the injection depth.

Well Sensitivities

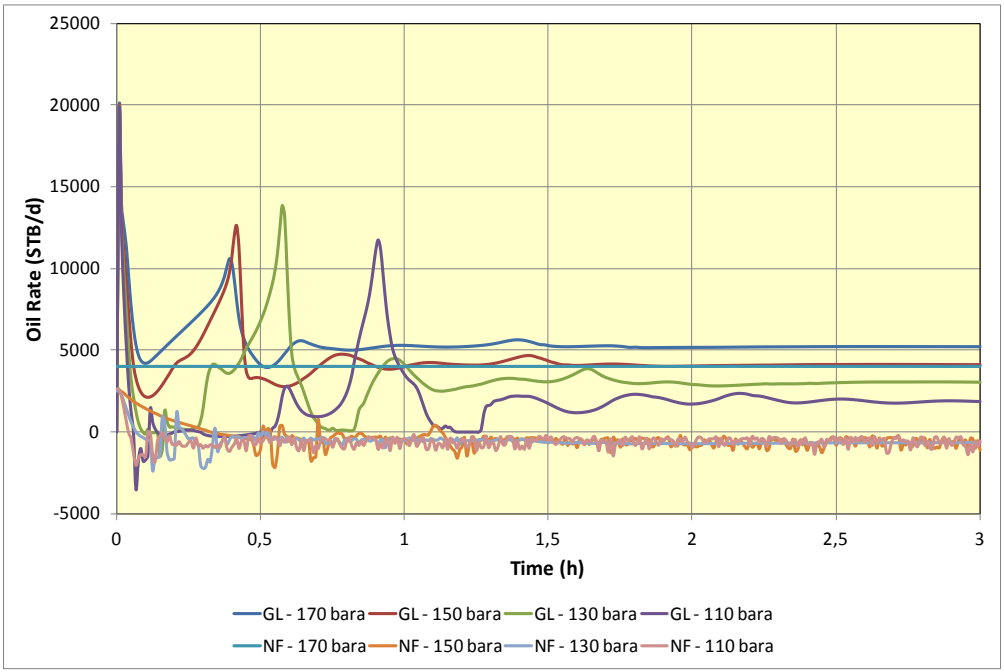

Figure 45 Oil rate of reservoir pressure sensitivity for with and without gas lift well

Figure 45 shows the oil production of the J-shaped well with and without gas lift at different reservoir pressure. Four reservoir pressure (170, 150, 130, 110 bara) are analyzed. Without gas lift, the S-02 well can be produced at the reservoir pressure higher than 170 bara. With gas lift, the S-02 well can be produced even the reservoir pressure of the well decreases down to 110 bara. However, Lower reservoir pressure in a gas lift well introduces longer static instability period. In terms of regularity, it demonstrates that gas lift can increase the regularity of wells with cyclic behavior.

Sensitivity of casing pressure is performed in order to analyze the effect of surface casing pressure (gas lift pressure) to the gas lift effectiveness. Figure 46 shows the gas lift injection rate in the casing at different casing pressure. Gas lift can be injected to the tubing when the gas lift pressure is above 120 barg. When the gas lift

pressure is below 110 barg, the gas lift is not able to be injected at the third gas lift mandrel since the tubing pressure is higher than the gas casing pressure at the injection depth. With the higher gas lift pressure, more gas is injected into the tubing until the critical gas lift rate is reached.

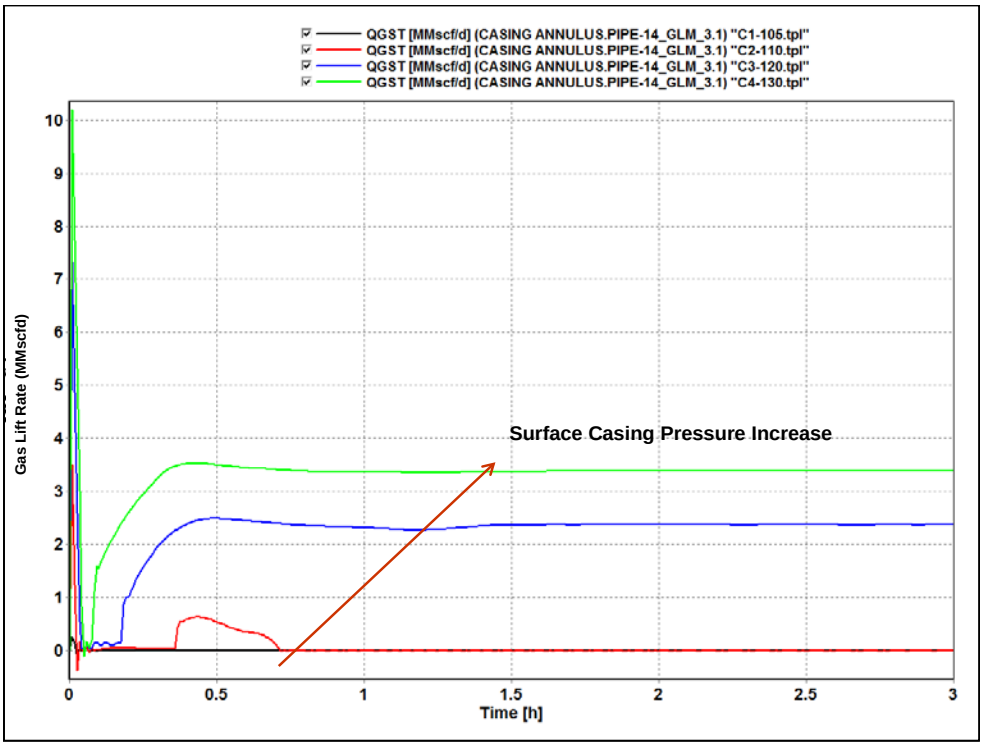

Figure 46 Gas lift injection rate at different surface casing pressure

Figure 47 shows the reservoir pressure sensitivities (210, 200, 190, 170, 150, 130, and 110 barg) for the gas lift well. The well can be produced even the reservoir pressure decreases down to 110 barg. The oil production behavior shows that the gas lift well can be produced at lower reservoir pressure. However, more fluctuation amplitude is observed during startup. Lower reservoir pressure in a gas lift well introduces longer static instability period. When the pressure is 210 barg, the static instability period is less than 2 hours. When the pressure decreases to 110 barg, the static instability period is nearly 4 hours.

Figure 48 shows the gas lift injection requirement at different reservoir pressure. The figure shows the gas lift injection requirement increases at lower reservoir pressure as a representative of the orifice type of gas lift valve performance curve. Reduced reservoir pressure introduces lower tubing pressure at the injection depth. However, the gas lift valve demonstrates the critical gas rate at 3.7 mmscfd.

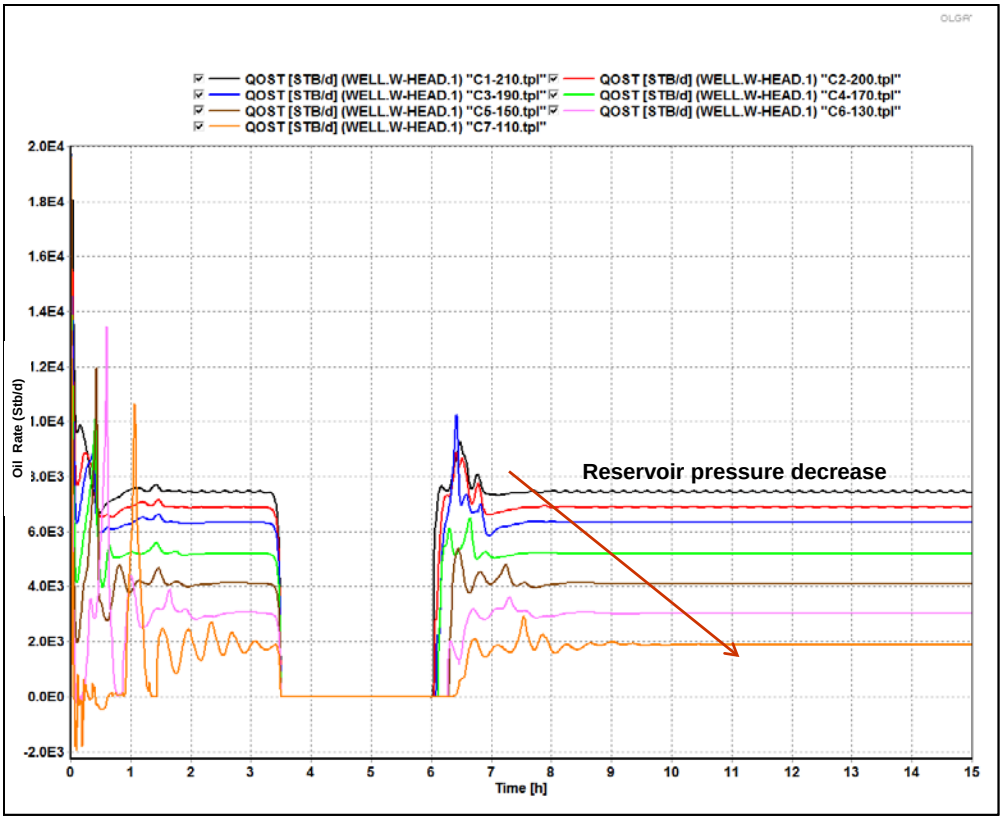

Figure 47 Oil production for reservoir pressure sensitivities in gas lift well

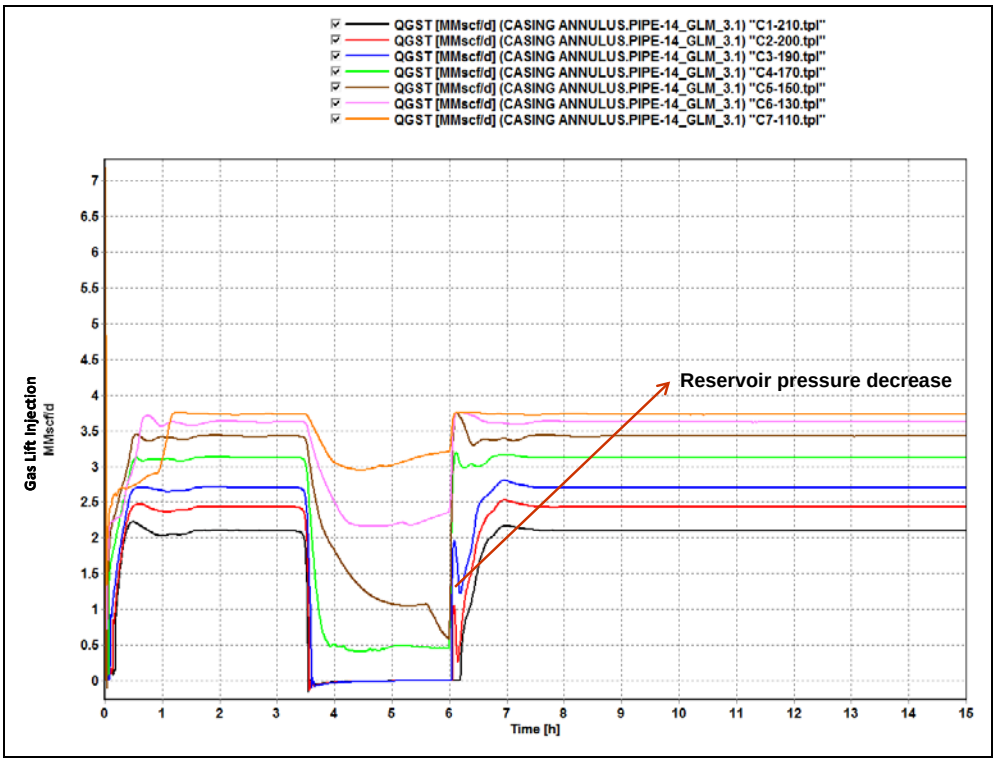

Figure 48 Gas lift injection for reservoir pressure sensitivities in gas lift well

Figure 49 shows sensitivity of the gas lift rate to the stability of the well. Gas lift rate is injected from 0 – 20 MMscfd. Surprisingly, the gas lift rate required to reach stable production is 15 MMscfd. From this figure, gas lift can be used to stabilize the slugging behavior. However, the required rate is extremely high. It shows that the high gas lift requirement change the fluid fraction along the well to be gas dominated. The gas dominated region mitigates the risk of oscillating sequence in the well production.

This phenomenon is in agreement with Pots[22] et al. who has done the analysis of instability in pipeline and riser. Pots suggests that gas lift reduces slugging but it required unrealistic large amount of gas. Pots also suggests that pipeline gas injection is more preferably than the riser injection to mitigate the instability.

However, high gas lift rate is not optimal in the multi-well system and integrated surface facility. High gas lift rate will increase the back pressure in the manifold pipeline. It can impact to the gas constraint and well capacity. The integrated system analysis , such as Integrated Production Modeling (IPM) analysis, is required to analyze this condition.

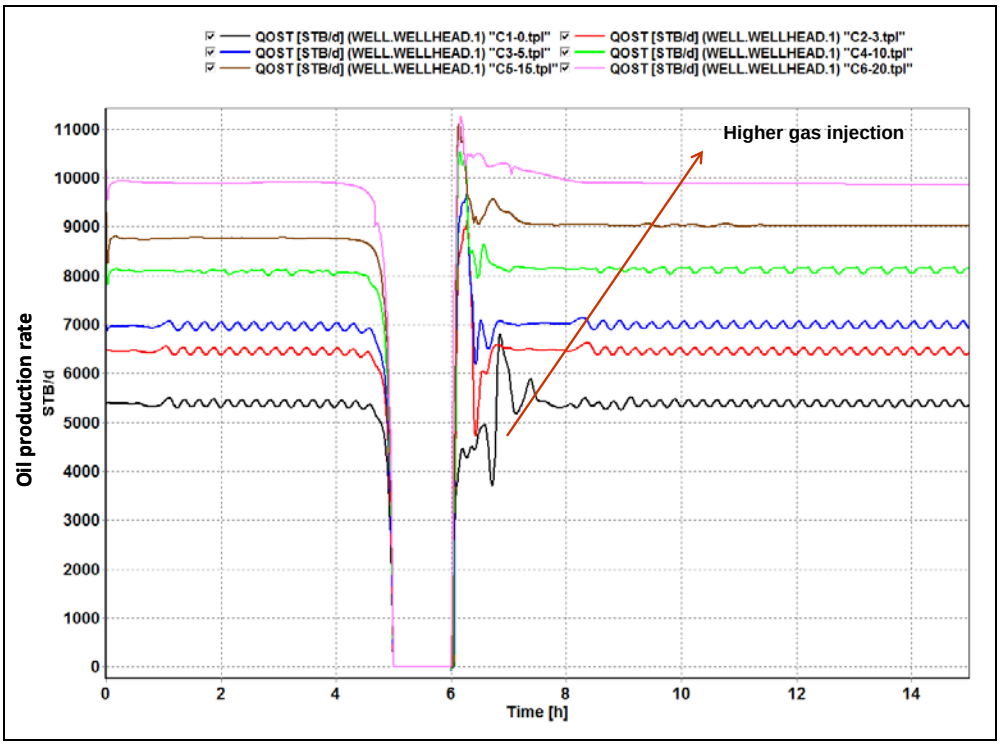

Figure 49 Gas lift injection sensitivities for stabilized gas lift well

4.2.3.5 Case #5 Gas Lift Injection after the Well is Shut In

Case #4 injects gas lift from the beginning of the well startup. Case #3 simulates the transient reservoir behavior where the well dies at certain reservoir pressure. Case #5 is the continuation of Case #3 where the gas lift is injected after the well dies. The objective of this case is to analyze the well behavior when the gas lift is injected. The gas lift is injected after the average reservoir pressure is not able to flow the well because of the high hydrostatic head in the wellbore. Case #3 shows that the well dies when the average reservoir pressure is around 160 bara.

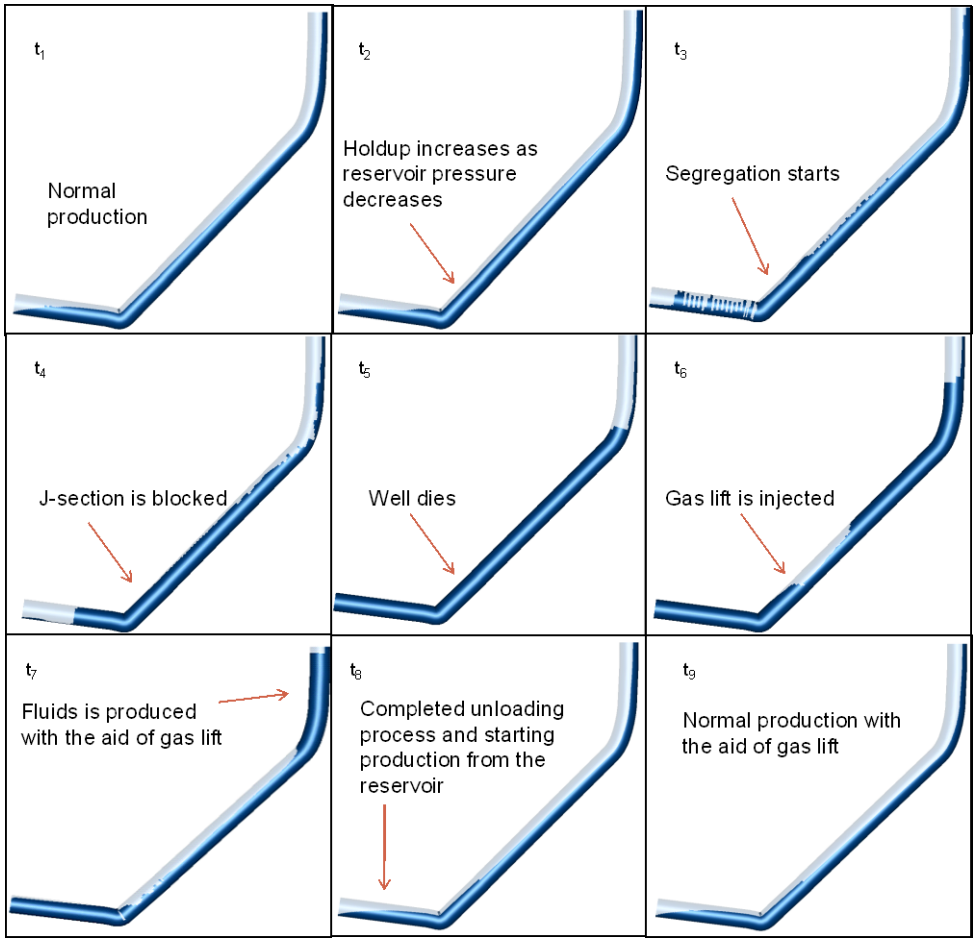

Figure 50 Holdup of shut in and gas lift behavior

The 2D holdup behavior below gives more understanding about the flow behavior along the gas lift injection. Figure 50 shows the behavior of the well during the decreasing of reservoir pressure and demonstrates the liquid behavior when the gas lift is injected at the lower reservoir pressure. The time t_1 until t_5 shows the liquid holdup behavior when the reservoir pressure decreases. Time t_6 to t_9 shows the

holdup behavior when the well is introduced by gas lift. At time t_1, the well is produced normally. At time t_2, the reservoir decreases, the liquid fraction along the tubing increases. However, the reservoir pressure is still high enough to produce the well. At time t_3, the fluid segregation occurs when the reservoir pressure is not sufficient to produce the well. The liquid is started to fill the J-section of the well. At time t_4, the J-section is blocked by the accumulation of the liquid. No production is observed in the wellhead. The liquid is accumulated in the bottom part of the well and the gas is accumulated in the upper part of the well. At time t_5, the well dies. Even the surface choke is in open position; no fluid is produced from the well. At time t_6, the gas is injected from the third gas lift mandrel. The accumulated liquid above the injection point is unloaded by the aid of gas lift. At time t_7, the liquid is produced and the gas lift injected is continued. The high gas lift injection during the unloading process causes some gas is observed flowing below the injection point. At time t_8, accumulated liquid above the injection point has been produced. The fluid from the reservoir is produced. Time t_9 shows the steady state well behavior where some oscillation amplitude is observed in the J-shaped well. In terms of reservoir pressure, gas lift can extend the lifetime of the well by reducing the mixing density of the fluid. The lower mixing density of the gas injection together with the fluid from the reservoir causes lower hydrostatic head above the injection point.

5 DISCUSSION

5.1 EFFECT OF WELL GEOMETRY

There are two cases that used for analyzing the effect of well geometry. Case #1 is the J-shaped well. Case #2 is the horizontal well. Comparison of the J-shaped well to the horizontal well geometry is analyzed to see the effect of well geometry to the well performance. Figure 51 shows the well geometries that used for both models including the reservoir section.

In terms of well performance, both wells can be produced at relatively similar rates. However, the J-shaped well demonstrate the presence of dynamic instability whereby oscillation amplitude is observed.

The downward inclination of the J-shaped well introduces periodic waves over time derived as a result of gas blowing over the surface. This behavior introduces periodic fluctuations of the superficial gas and liquid velocity in the J-shaped well along the depth. This behavior has an indication to slugging behavior.

Reservoir pressure sensitivity for both well types demonstrates more difficulties during startup of the J-shaped well at low reservoir pressure. In J-shaped wells, higher oscillation amplitudes are observed due to high water cut.

The J-shaped well demonstrates unfavorable behavior compare to horizontal well. The J-shaped well has prone to slugging.

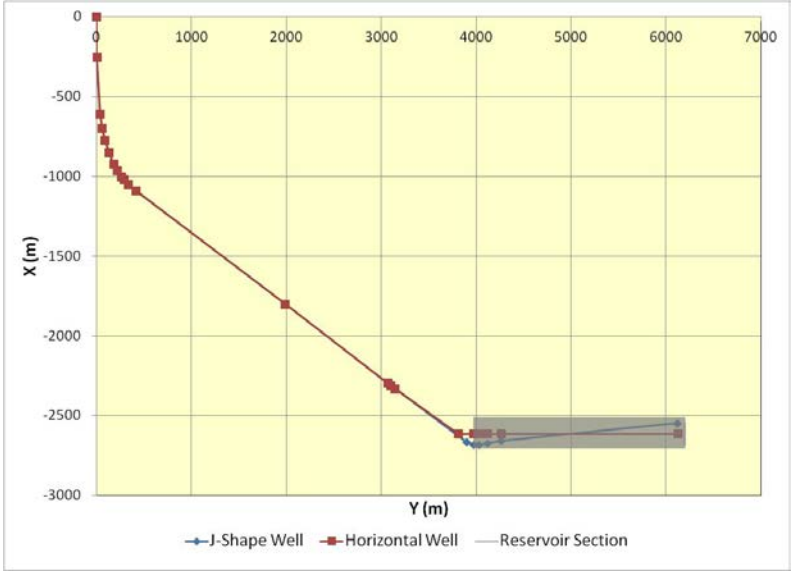

Figure 51 Well geometry for J-shaped and horizontal well

5.2 EFFECT OF GAS LIFT

Gas lift design is performed using Prosper. Steady state simulation (Prosper) utilized currently is to do classical gas lift design. OLGA uses the gas lift design as a result from Prosper simulation. OLGA is used for validation purposes. OLGA can analyze the dynamic well behavior based on the gas lift design from Prosper. OLGA can analyze the details well parameter in order to understand the vertical lift performance in the J-shaped well. Combination of steady state and dynamic simulation is an opportunity to establish better gas lift design. In this thesis, OLGA is used to analyze the details dynamic well behavior during gas lift operation.

The gas lift operation affects the mixing density between the gas lift injection and the fluid from the reservoir. Lower density above the gas lift injection depth lowers the fluid gradient along the well. Gas lift establishes lower bottomhole pressure at the injection depth than the natural flowing well. Gas lift bottomhole pressure is lower than the bottomhole pressure of the natural flowing well. Lower bottomhole pressure at the gas lift well establishes higher drawdown that increases the flow rate of the well.

The mixing density above the gas lift injection depth also affects the pressure drop along the tubing. This behavior is confirmed by the liquid fraction (holdup) distribution along the well. It tells that the liquid is accumulated at the bottom part of the well. Gas lift injection lowers the liquid fraction along the tubing above the injection point. The lower liquid fraction exhibits lower pressure drop along the wellbore. The lower pressure drop in a gas lift well establishes higher wellhead pressure at the surface and/or lower bottomhole pressure. In the model, lower bottomhole pressure is observed since it assumed that the wellhead pressure is similar. In the actual behavior, Figure 12 shows that the higher wellhead pressure is observed even it is difficult to see the change in the bottomhole pressure (see Figure 11).

Sensitivity of surface casing pressure is performed to see the effect of the surface casing pressure to the effectiveness of gas lift operation. Certain surface casing pressure needs to be achieved to ensure that the casing pressure is higher than the tubing pressure at the injection depth.

In terms of well lifetime, gas lift can extend the life of the field in terms of producing at the lower reservoir pressure. At the lower reservoir pressure, gas lift can help to produce the well but the risk of unstable behavior is higher. The effectiveness of gas lift is not seen in high reservoir pressure and low water cut. When the reservoir pressure decreases and the water starts to produce, the effectiveness of gas lift increases.

5.3 STARTUP PERFORMANCE

Startup behavior is analyzed by studying the well behavior after shut in period. The shut-in models the fluid segregation along the well. When the well is opened, static instability is observed by some fluctuation during fluid unloading. More fluctuation is observed at low reservoir pressure, low productivity index and high water cut.

Well startup behavior for the J-shaped and horizontal well is compared in order to analyze the effect of well geometry to the well startup. The J-shaped well shows more fluctuation behavior compared to the horizontal well.

Startup can be difficult at low reservoir pressure and high water cut. Based on the steady state calculation, the well can be produced at the low reservoir pressure. However, when the fluid segregation is modeled during shut in period, it is difficult to startup the well. The liquid is accumulated and result liquid blockage. To properly evaluate the possibility of producing well without the aid of gas lift, it is recommended to simulate the segregation during shut in and following by startup/unloading sequence. Otherwise, the steady state simulation result can be misleading because it does not model the dynamic/transient behavior during unloading.

Better startup performance is seen in the gas lift well. With gas lift, static instability period is less than the well produced naturally. In terms of reservoir pressure, gas lift well can be produced at the lower reservoir pressure than the natural flowing well. However, Lower reservoir pressure in a gas lift well introduces longer static instability period.

Gas lift injection at the lower reservoir pressure seems to be more effective than at the higher reservoir pressure. In the actual condition, the gas lift at least can increase the regularity of the cyclical basis in this well.

In terms of gas lift design, steady state simulation is the standard technique that currently utilized to do classical gas lift design. Dynamic/transient simulation is recommended for validation purposes of gas lift design intended for wells with complex well geometry. Modeling shall be implemented in the future to engineer/design gas lift solution for wells with complex well geometry.

5.4 WELL INSTABILITY

Well instability is analyzed in this study. In dynamic simulation, the static and dynamic instabilities are analyzed by understanding well behavior during startup and stable production. The pressure, flow rate, liquid fraction, and flow regime are the parameters that are analyzed to understand the instabilities. The liquid fraction behavior along the well is very useful to explain the effect of decreasing reservoir pressure for the gas lift well and the startup of gas lift well

behavior. It is also possible to predict a period of time during static instability using dynamic simulation. In this study, the static instability is seen during the startup of the well. The high fluctuation of the oil rate is shown at the beginning of the startup. This can be mitigated by opening the well gradually. The oscillation amplitudes are also included as well instability as shown by the behavior of the J-shaped well. This instability is clearly seen because of the downward inclination of the J-section of the well. Dynamic instability is also seen by comparing both of the flow regime at the wellhead and the bottomhole (gauge) depth position to predict the transition from bubble to slug flow. From this analysis, slugging behavior is observed in this analysis

In terms of stability, the gas lift well can mitigate the instability. However, the large amount of gas lift is required to stabilize the slug flow. Occasionally, high gas lift rate is not optimal in the multi-well system and integrated surface facility. High gas lift rate will increase the back pressure in the manifold pipeline that can restrict the fluid flow from other wells. The integrated system analysis, such as Integrated Production Modeling (IPM) analysis, is required to analyze this condition.

5.5 TRANSIENT RESERVOIR BEHAVIOR

The effect of the transient reservoir behavior is analyzed in this study. The fact that there is a decreasing of the bottomhole pressure during 20 days of production shows that the well behavior indicates in the transient behavior. The dynamic simulation is used to model this condition. Decreasing of the reservoir pressure during production period is used as a parameter that represents the actual reservoir pressure in the near wellbore area. The decreasing of the reservoir is observed until the well is shut in. The increasing of the reservoir pressure during the shut in time represents the build up pressure at the near wellbore area.

The effect of the transient reservoir behavior started when the hydrostatic head increases until the well is shut in. When the reservoir pressure decreases, the liquid fraction along the well increases until the well dies. When the well is shut in, the reservoir pressure builds until certain pressure. Since this well has relatively strong transient reservoir behavior, the buildup of reservoir pressure takes quite long time. When the average reservoir pressure is sufficient to handle the hydrostatic heading, the well will be produced for certain period.

The transient reservoir behavior simulation shows that the well can be produced at the lower reservoir pressure than the required reservoir pressure for well start up.

With the help of gas lift, the last simulation shows that gas lift can extend the lifetime of well with strong transient reservoir behavior.

6 CONCLUSIONS

The conclusions of this study are summarized as below:

- The J-shaped well demonstrates unfavorable behavior compare to horizontal well. The J-shaped well has prone to slugging behavior.
- To properly evaluate the possibility of producing a well without the aid of gas lift, it is recommended to simulate the segregation during shut in and following by startup/unloading sequence. Otherwise, the steady state simulation result can be misleading because it does not model the dynamic behavior during unloading.
- Gas lift can extend the lifetime of well with strong transient reservoir behavior. Gas lift can increase the regularity wells with cyclic behavior.
- In terms of stability, gas lift well can mitigate the instability. However, a large amount of gas lift is required to stabilize the flow.
- Steady state simulation is currently the standard technique utilized to do classical gas lift design. Dynamic/transient simulation is recommended for validation purposes of gas lift design intended for wells with complex well geometry. Modeling shall be implemented in the future to engineer/design gas lift solution for wells with complex well geometry.

7 REFERENCES

1) Asheim, H.: “Criteria for Gas-Lift Stability”, JPT Nov 1988, pp1452 – 1456

2) Z. G. Xu and M. Golan,.:”Criteria for Operation Stability of Gas Lift Wells”, SPE 019362, 1989

3) Bertuzzi, A. F., Welchon, J.K., Poettmann, F. H.:”Description and Analysis of an Efficient Continuous-Flow Gas-Lift Installation”, SPE 953271, 1953

4) Decker, K. L., “Gas-Lift Valve Performance Testing”, SPE 25444, 1993

5) Decker, K. L. “ IPO Gas Lift with Valve Performance”, SPE 109694, 2008

6) Hu, B., Golan, M., “Gas-lift Instability Resulted Production Loss and Its Remedy by Feedback Control: Dynamical Simulation Results”, SPE 84917, 2003

7) Norris III, H. L., ”Tutorial – Current Topics in Vapour-Liquid Multiphase Flow”, PSIG Annual Meeting, El-Paso, 1989

8) Gilbert, W. E., “Flowing and Gas Lift Well Performance”, Pacific Coast District, Division of Production, Los Angeles, May 1954

9) Calvert, Patrick and Guevara, Ernesto., Appraisal of the Valhall Gas-Lift System, BP - Internal Report, August 2010

10) Pucknell, J. K., Goodbrand, Shona., Green, A. S., “Solving Gas Lift Problems in the North Sea Clyde’s Field”, SPE 28915, 1994

11) Sinegre, Laure., Petit, Nicolas., and Menegatti, Philippe,., “Predicting Instabilities in Gas-lifted Wells Simulation”, Proceedings of 2006 American Control Conference Minneapolis, Minnesota, USA, page. 5530 – 5537, 2006

12) Faustinelli, Juan., Bermudez, Gaston., and Cuauro, Antonio., “A Solution to Instability Problems in Continuous Gas-Lift Wells Offshore Lake Maracaibo”, SPE 53959, 1999

13) Asheim, H., “Verification of Transient, Multi-Phase Flow Simulation for Gas Lift Applications”, SPE 56659, 1999

14) Malekzadeh, R., Mudde, R.F., “Modeling Study of Severe Slugging”, SPE-150364, February 2012.

15) Takacs, Gabor., “Gas Lift Manual”, PennWell, 2005

16) Alhanati, F.J.S., Schmidt, Zelimir., and Doty, D.R., Continuous Gas-Lift Instability: Diagnosis, Criteria, and Solutions”, SPE 26554, 1993

17) Calvert, P., Davis, J., “A Dynamic Business Needs Dynamic Solutions; How Field of the Future Has Turned BP into a Smooth Operator”, SPE 128682, 2010

18) Havre, K., Dalsmo, M., “Active Feedback Control as a Solution to Severe Slugging”, SPE 79252, 2002

19) Jossi, S.D., “Augmentation of Well Productivity with Slant and Horizontal Wells”, JPT, 729-739, June 1988

20) Economides, M. J., Deimbacher, F.X., Brand, C.W., and Heinemann,Z. E., “Comprehensive Simulation of Horizontal Well Performance”, SPE 20717, 1990, and SPEFE, 418 – 426, December 1991.

21) Jansen, F.E., “A Study on the Optimization of Severe Slugging Elimination”, SPE 22328, 1991.

22) Pots, B.F.M., Bromilov, I.G., Konijn, M.J.W.F., “Severe Slug Flow in Offshore Flowline /Riser Systems”, SPE 13723, November 1987

23) Petroleum Technology Company, “Gas Lift Design BP Valhall S-2”, Internal Report, 14 June 2010

8 NOMENCLATURE

A_1 : injection port size, m^2 [ft^2]

B_g : Formation Volume Factor of gas at injection point

D : vertical depth to injection point, m [ft]

E : orifice efficiency factor, here assumed to equal 0.9

F_1 : 1^{st} order of stability criteria

F_2 : 2^{nd} order of stability criteria

g : acceleration of gravity, m/s^2 [ft/sec^2)

J : productivity index, std m^3/s.Pa [scf/sec.psi]

P_p : pipeline pressure, Pa [psi]

P_r : riser pressure, Pa [psi]

p_t : tubing pressure, Pa [psi]

q_{fi} : flow rate of reservoir fluids at injection point, m^3/s [ft^3/sec]

q_{gi} : flow rate of lift gas at injection point, m^3/s [ft^3/sec]

q_{gsc} : flow rate of lift gas at standard conditions, std m^3/s [scf/sec]

q_{Lsc} : flow rate of liquids at standard conditions, std m^3/s [scf/sec]

V_t : tubing volume downstream of gas injection point, m^3 [ft^3]

V_c : gas conduit volume, m^3 [ft^3]

ρ_{fi} : reservoir fluid density at injection point, kg/m^3[lbm/ft^3]

ρ_{gi} : lift-gas density at the injection point, kg/m^3[lbm/ft^3]

ρ_{gsc} : lift-gas density at standard surface conditions, kg/std m^3[lbm/scf]

9 APPENDIX

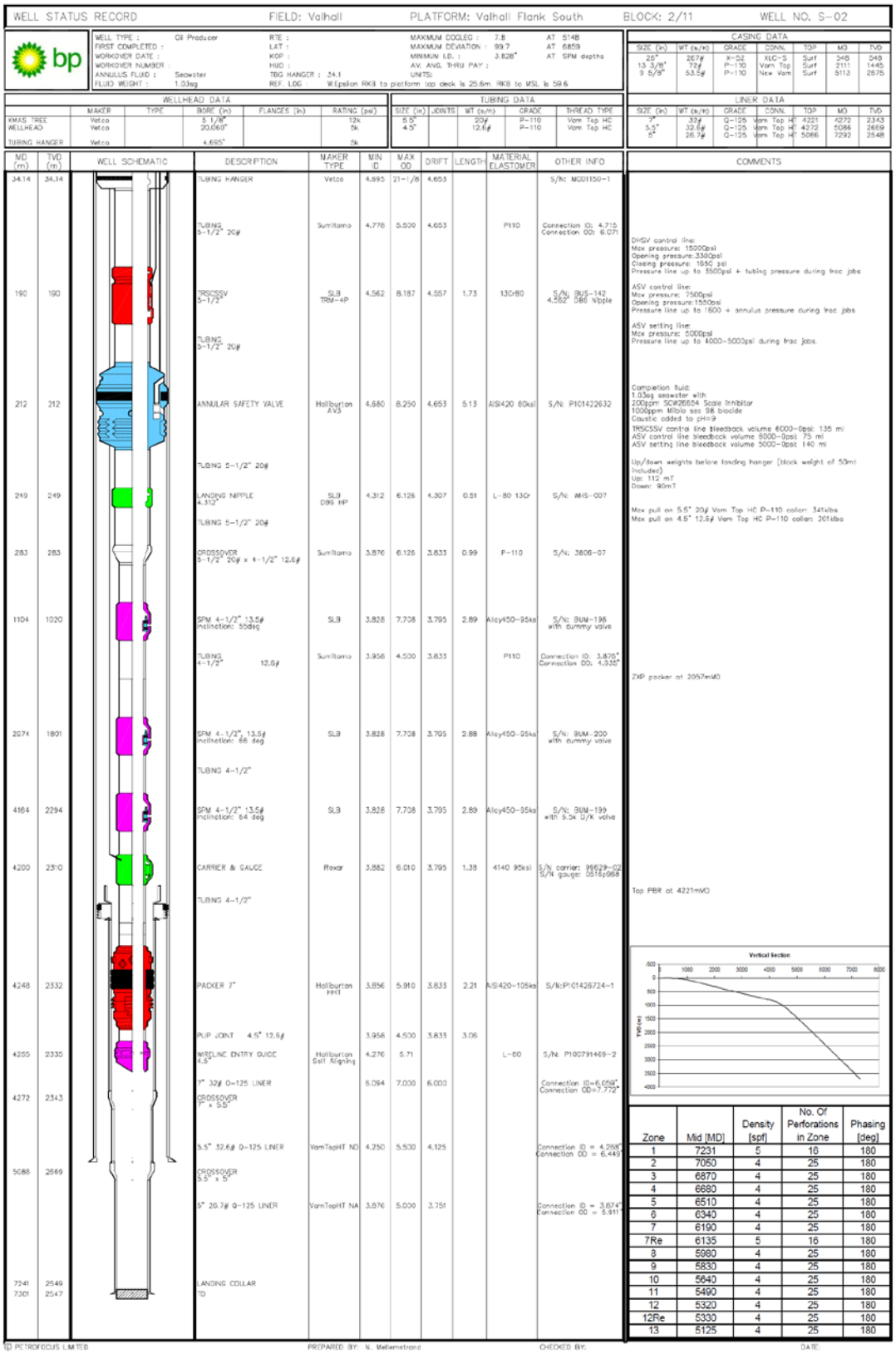

Figure A. 1 S-02 Wellbore Schematic

Table A. 1 Well Geometry of J-shaped Well in OLGA

Pipe	x [m]	y [m]	Length [m]	Elevation [m]	# Sections	Length of sections (list [m])	Diameter [m]	Roughness [m]
Start Point	6118,06	-2547,39						
PIPE-2_BH	4259,04	-2657,74	1862	-110,35	40	40:46,6	0,098451	1,52E-05
PIPE-3	4114,89	-2671,49	145	-13,75	6	06:24,1	0,098451	1,52E-05
PIPE-4	4029,71	-2681,78	86	-10,29	3	03:28,6	0,098451	1,52E-05
PIPE-5	3970,01	-2681,14	60	0,64	2	02:29,9	0,10795	1,52E-05
PIPE-6	3897,34	-2665,19	74	15,95	2	02:37,2	0,154788	1,52E-05
PIPE-7	3141,53	-2332	826	333,19	18	18:45,9	0,100533	1,52E-05
Gauge Depth	3098,87	-2310	48	22	2	02:24,0	0,100533	1,52E-05
PIPE-9_GLM_3	3066,62	-2294	36	16	2	02:18,0	0,100533	1,52E-05
PIPE-10_GLM_2	1983,54	-1801	1190	493	36	36:33,1	0,100533	1,52E-05
PIPE-11	410,475	-1088,75	1727	712,25	36	36:48,0	0,100533	1,52E-05
PIPE-12	333,113	-1050,73	86	38,02	3	03:28,7	0,100533	1,52E-05
PIPE-13_GLM_13	285,106	-1020	57	30,73	2	02:28,5	0,100533	1,52E-05
PIPE-14	259,778	-1001,61	31	18,39	2	02:15,7	0,100533	1,52E-05
PIPE-15	217,227	-964,44	56	37,17	2	02:28,3	0,100533	1,52E-05
PIPE-16	177,858	-921,44	58	43	2	02:29,2	0,100533	1,52E-05
PIPE-17	128,377	-850,49	87	70,95	2	02:43,3	0,100533	1,52E-05
PIPE-18	86,9637	-774,89	86	75,6	2	02:43,1	0,100533	1,52E-05
PIPE-19	55,425	-695,85	85	79,04	2	02:42,5	0,100533	1,52E-05
PIPE-20	34,1104	-612,43	86	83,42	2	02:43,0	0,121361	1,52E-05
PIPE-21	0,446654	-249,99	364	362,44	6	07:00,7	0,121361	1,52E-05
Wellhead	0	0	250	249,99	4	05:02,5	0,121361	1,52E-05

Table A. 2 Well Geometry of Horizontal Well in OLGA

Pipe	x [m]	y [m]	Length [m]	Elevation [m]	# Sections	Length of sections (list [m])	Diameter [m]	Roughness [m]
Start Point	6124,06	-2614,54						
B-Hole	4259,04	-2614,55	1865	-0,01	40	40:46,6	0,098451	1,52E-05
PIPE-3	4114,89	-2614,56	144	-0,01	6	06:24,0	0,098451	1,52E-05
PIPE-4	4029,71	-2614,57	85	-0,01	3	03:28,4	0,098451	1,52E-05
PIPE-5	3970,01	-2614,58	60	-0,01	2	02:29,9	0,10795	1,52E-05
PIPE-6	3812,09	-2614,59	158	-0,01	4	04:39,5	0,154788	1,52E-05
PIPE-7	3141,53	-2332	728	282,59	16	16:45,5	0,100533	1,52E-05
Gauge Depth	3098,87	-2310	48	22	2	02:24,0	0,100533	1,52E-05
GLM_3	3066,62	-2294	36	16	2	02:18,0	0,100533	1,52E-05
GLM_2	1983,54	-1801	1190	493	36	36:33,1	0,100533	1,52E-05
PIPE-11	410,475	-1088,75	1727	712,25	36	36:48,0	0,100533	1,52E-05
PIPE-12	333,113	-1050,73	86	38,02	3	03:28,7	0,100533	1,52E-05
GLM_13	285,106	-1020	57	30,73	2	02:28,5	0,100533	1,52E-05
PIPE-14	259,778	-1001,61	31	18,39	2	02:15,7	0,100533	1,52E-05
PIPE-15	217,227	-964,44	56	37,17	2	02:28,3	0,100533	1,52E-05
PIPE-16	177,858	-921,44	58	43	2	02:29,2	0,100533	1,52E-05
PIPE-17	128,377	-850,49	87	70,95	2	02:43,3	0,100533	1,52E-05
PIPE-18	86,9637	-774,89	86	75,6	2	02:43,1	0,100533	1,52E-05
PIPE-19	55,425	-695,85	85	79,04	2	02:42,5	0,100533	1,52E-05
PIPE-20	34,1104	-612,43	86	83,42	2	02:43,0	0,121361	1,52E-05
PIPE-21	0,446654	-249,99	364	362,44	6	07:00,7	0,121361	1,52E-05
W-Head	0	0	250	249,99	4	05:02,5	0,121361	1,52E-05

Table A. 3 Annulus Geometry of Gas Lift Well in OLGA

Pipe	x [m]	y [m]	Length [m]	Elevation [m]	# Sections	Length of sections (list [m])	Diameter [m]	Roughness [m]
Start Point	-12	0						
PIPE-1	0	0	12	0	2	06:00,0	0,077089	1,00E-05
PIPE-2	0,446654	-249,99	250	-249,99	21	21:11,9	0,077089	1,00E-05
PIPE-3	34,1104	-612,43	364	-362,44	16	16:22,8	0,102489	1,00E-05
PIPE-4	55,425	-695,85	86	-83,42	2	02:43,0	0,102489	1,00E-05
PIPE-5	86,9637	-774,89	85	-79,04	2	02:42,5	0,102489	1,00E-05
PIPE-6	128,377	-850,49	86	-75,6	2	02:43,1	0,102489	1,00E-05
PIPE-7	177,858	-921,44	87	-70,95	2	02:43,3	0,102489	1,00E-05
PIPE-8	217,227	-964,44	58	-43	2	02:29,2	0,102489	1,00E-05
PIPE-9	259,778	-1001,61	56	-37,17	2	02:28,3	0,102489	1,00E-05
PIPE-10_GLM_1	285,106	-1020	31	-18,39	2	02:15,7	0,102489	1,00E-05
PIPE-11	333,113	-1050,73	57	-30,73	2	02:28,5	0,102489	1,00E-05
PIPE-12	410,475	-1088,75	86	-38,02	3	03:28,7	0,102489	1,00E-05
PIPE-13_GLM_2	1983,54	-1801	1727	-712,25	36	36:48,0	0,102489	1,00E-05
PIPE-14_GLM_3	3066,62	-2294	1190	-493	36	36:33,1	0,102489	1,00E-05

Table A. 4 J-Shaped Well input data in OLGA

No				1
Name				J-shape Well
PVT				S-02 OLGA Well
Integration			End Time (h)	15
OPTION			Temperature	Ugiven
			Steady State	On
Flowpath : Well	Boundary & Initial Condition	Heat Transfer	Interpolation	Vertical
			INTAMBIENT (°C)	93
			OUTTAMBIENT (°C)	5
			Uvalue (W/m2-C)	10
		Zone	Prodoption	Linear
			Injoption	Linear
			Respressure (bara)	210
			Restemperature (°C)	93
			Time	0
			WC	0
			GORST (SCF/STB)	1000
			Position	Bottom Perf to Top Perf
			Injectivity (STB/d/psi)	8
			Prodi (STB/d/psi)	11
	Output	Profile Data	Variable	ID, DPZF, DPZG, HOL, PT, QGST, QOST, TM, USG, USLTHL
		Trend Data	Variable	ID, DPZF, DPZG, HOL, PT, QGST, QOST, TM, USG, USLTHL
			Pipe	PIPE-9_GLM_3, GAUGE DEPTH, WELLHEAD
	Process Equipment	Valve	Label	Surface Choke
			Model	Hydrovalve
			Opening Time (hrs)	0, 3, 3.01, 6, 6.01, 15
			Opening	2:1, 2:0, 2:1
			Diameter (m)	0.121361
		Position	Pipe	WELLHEAD
			Section Boundary	1
Node		B-Hole	Type	Closed
			Fluid	S-02 OLGA Well
		W-Head	Type	Pressure
			Fluid	S-02 OLGA Well
			Gas Fraction	-1
			Temperature (°C)	15
			Pressure (bara)	30

Table A. 5 Horizontal Well input data in OLGA

No				2
Name				Horizontal Well
PVT				S-02 OLGA Well
Integration			End Time (h)	15
OPTION			Temperature	Ugiven
			Steady State	On
Flowpath : Well	Boundary & Initial Condition	Heat Transfer	Interpolation	Vertical
			INTAMBIENT (°C)	93
			OUTTAMBIENT (°C)	5
			Uvalue (W/m2-C)	10
		Zone	Prodoption	Linear
			Injoption	Linear
			Respressure (bara)	210
			Restemperature (°C)	93
			Time	0
			WC	0
			GORST (SCF/STB)	1000
			Position	Bottom Perf to Top Perf
			Injectivity (STB/d/psi)	8
			Prodi (STB/d/psi)	11
	Output	Profile Data	Variable	ID, DPZF, DPZG, HOL, PT, QGST, QOST, TM, USG, USLTHL
		Trend Data	Variable	ID, DPZF, DPZG, HOL, PT, QGST, QOST, TM, USG, USLTHL
			Pipe	B-HOLE, GAUGE DEPTH, GLM_3, W-HEAD
	Process Equipment	Valve	Label	Surface Choke
			Model	Hydrovalve
			Opening Time (hrs)	0, 3, 3.01, 6, 6.01, 15
			Opening	2:1, 2:0, 2:1
			Diameter (m)	0.121361
		Position	Pipe	W-HEAD
			Section Boundary	1
Node		B-Hole	Type	Closed
			Fluid	S-02 OLGA Well
		W-Head	Type	Pressure
			Fluid	S-02 OLGA Well
			Gas Fraction	-1
			Temperature (°C)	15
			Pressure (bara)	30

Table A. 6 Transient behavior model input data in OLGA

No				3
Name				Transient Behavior Model
PVT				S-02 OLGA Well
Integration			End Time (d)	**24**
OPTION			Temperature	Ugiven
			Steady State	On
Flowpath : Well	Boundary & Initial Condition	Heat Transfer	Interpolation	Vertical
			INTAMBIENT (°C)	93
			OUTTAMBIENT (°C)	5
			Uvalue (W/m2-C)	10
		Well	Prodoption	Linear
			Injoption	Linear
			Respressure (bara)	200, 190, 180, 170, 160
			Restemperature (°C)	5:93
			Time (d)	0, 3, 9, 18, 24
			WC	5:0
			GORST (SCF/STB)	5:1000
			Position	Pipe-2_BH ; 1
			Injectivity (STB/d/psi)	14:8
			Prodi (STB/d/psi)	5:11
		Profile Data	Variable	ID, DPZF, DPZG, HOL, PT, QGST, QOST,TM, USG, USLTHL
		Trend Data	Variable	ID, DPZF, DPZG, HOL, PT, QGST, QOST,TM, USG, USLTHL
			Pipe	PIPE-2_BH, PIPE-8_GAUGE, PIPE-9_GLM_3, PIPE-10_GLM_2, PIPE-13_GLM_13, PIPE-23_WH
	Process Equipment	Valve	Label	Surface Choke
			Model	Hydrovalve
			Opening Time (hrs)	0, 3, 3.01, 6, 6.01, 15
			Opening	2:1, 2:0, 2:1
			Diameter (m)	0.121361
		Position	Pipe	Pipe-23_WH
			Section Boundary	1
Node		B-Hole	Type	Closed
			Fluid	S-02 OLGA Well
		W-Head	Type	Pressure
			Fluid	S-02 OLGA Well
			Gas Fraction	-1
			Temperature (°C)	15
			Pressure (bara)	30

Table A. 7 Gas lift model input data in OLGA

No				4
Name				Gas Lift
PVT				S-02 OLGA Well
Integration			End Time (h)	15
OPTION			Temperature	Ugiven
			Steady State	On
Flowpath : Well	Boundary & Initial Condition	Heat Transfer	Interpolation	Vertical
			INTAMBIENT (°C)	93
			OUTTAMBIENT (°C)	5
			Uvalue (W/m2-C)	10
	Output	Profile Data	Variable	ID, DPZF, DPZG, HOL, PT, QGST, QOST, TM, USG, USLTHL
		Trend Data	Variable	ID, DPZF, DPZG, HOL, PT, QGST, QOST, TM, USG, USLTHL
			Pipe	B-HOLE, GAUGE DEPTH, GLM_3, W-HEAD
	Position	Position	Label	GAS-To
			Pipe	Pipe-8_GLM_3
			Section	1
	Process Equipment	Valve	Label	Surface Choke
			Model	Hydrovalve
			Opening Time (hrs)	0, 3, 3.01, 6, 6.01, 15
			Opening	2:1, 2:0, 2:1
			Diameter (m)	0.121361
		Position	Pipe	Pipe-21_WH
			Section Boundary	1
Flowpath : Casing Annulus	Boundary & Initial Condition	Heat Transfer	Interpolation	Vertical
			INTAMBIENT (°C)	5
			OUTTAMBIENT (°C)	60
			Uvalue (W/m2-C)	10
		Profile Data	Variable	HOL, ID, PT, QGST, QOST, TM, USG, USLTHL
		Trend Data	Variable	HOL, ID, PT, QGST, QOST, TM, USG, USLTHL
			Pipe	B-HOLE, GAUGE, GLM_3, W-HEAD
	Process Equipment	Valve	Label	Gas Lift Choke
			Model	Hydrovalve
			Opening Time (hrs)	0, 3, 3.01, 6, 6.01, 15
			Diameter (in)	2
			Opening	2:1, 2:0, 2:1
			Pipe	Pipe-1
			Section Boundary	1
		Leak	Label	GLV
			Valve Type	GASLIFTVALVE
			Top Position	Gas-To
			Check Valve	YES
			Pipe	Pipe-14
			Section Boundary	36
			Gas Lift Valve	Demo GLV
			Choke Size	-1
			Port Size (1/64th)	20
			Correlation	VPClimited
Node		B-Hole	Type	Closed
			Fluid	S-02 OLGA Well
		Casing Head	Type	Pressure
			Fluid	S-02 OLGA Well
			Total Water Fraction	-1
			Gas Fraction	1
			Temperature (°C)	5
			Pressure (bara)	108
			WATER CUT	-1
		Packer	Type	Closed
			Fluid	S-02 OLGA Well
		W-Head	Type	Pressure
			Fluid	S-02 OLGA Well
			Gas Fraction	-1
			Temperature (°C)	15
			Pressure (bara)	30